

Portable Oxygen Device Design: Membrane and Pressure Swing Adsorption Technology Alternatives and Market Analysis

Technical Report Submitted to:
Dr. Miguel Bagajewicz
University of Oklahoma
School of Chemical, Biological, and Materials Engineering

Capstone Design Project Spring 2005

Adam Bortka
T. J. Chancellor
Jon Demster
Ashlee Ford
Eli Kliewer
Kara Shelden

May 2, 2005

Table of Contents

List of Figures and Tables.....	3
1.0 Executive Summary	4
2.0 Design Motivation	5
2.1 Introduction to Oxygen Therapy.....	5
2.1.1 Oxygen Therapy Use	5
2.1.2 Medical Insurance Coverage.....	6
2.2 Existing Oxygen Therapy Devices	7
2.2.1 Compressed Oxygen Tanks	7
2.2.2 Liquid Oxygen Tanks	8
2.2.3 Oxygen Concentrators	9
3.0 Membrane Gas Separation Technology.....	11
3.1 Introduction to Membranes.....	11
3.2 Ionic Ceramic Oxide Membranes	13
3.2.1 Principles.....	13
3.2.2 Materials	14
3.2.3 Modeling of Membrane Performance	14
4.0 Ionic Ceramic Membrane Design Results	15
5.0 Description of Device Components.....	16
5.1 Membrane Stack	17
5.2 Heating Element	20
5.3 Sealant.....	21
5.4 Heat Exchanger.....	24
5.4.1 Heat Exchanger Background	24
5.4.2 Heat Exchanger Design.....	25
5.5 Insulation	29
5.5.1 Radiation Heat Shielding.....	30
5.5.2 Cell External Insulation	30
5.6 Feed Pump	32
5.7 Power Supply	33
5.8 Controllers	34
5.9 External Casing.....	34
5.10 Prototype Cost.....	35
6.0 Pressure Swing Adsorption.....	36
6.1 Theory	36
6.2 Model Performance.....	39
6.2.1 Nitrogen Removal.....	39
6.2.2 Argon Removal.....	41
6.3 Column Sizing	44
6.4 Practicality of Device.....	45
6.5 Bottling Device.....	46
6.6 Compressors.....	47
6.7 Air Drying.....	48
6.8 Materials	49
7.0 Marketing and Cost Analysis.....	52
7.1 Price Determination	52

7.1.1 The Alpha Function	53
7.1.2 The Beta Function.....	54
7.1.3 Happiness Determination.....	55
7.1.4 Demand as a Function of Selling Price.....	57
7.2 Correcting the Model Error and Results	58
8.0 Device Approval Regulations.....	60
8.1 FDA Regulations	60
8.2 FAA Regulations	62
9.0 Conclusion	63
References.....	63
Supporting Materials.....	66
Appendix A1-Polymer Membranes Background.....	67
A1.1 Principles.....	67
A1.2 Materials	67
Appendix A2-Polymer Membrane Models.....	68
A2.1 Mixed Flow Polymer Model.....	70
A2.2 Counter-Current Polymer Model.....	73
A2.3 Cascade Model.....	76
Appendix A3-Polymer Membrane Design Results.....	76
A3.1 Oxygen Separation from Air.....	76
A3.2 Removal of Argon from 95% Oxygen PSA Product Stream.....	77
Appendix B1-Mixed Conducting Ceramic Oxide Membrane Background	79
B1.1 Principles.....	79
B1.2 Materials.....	80
Appendix B2-Mixed Conducting Ceramic Oxide Model.....	80
Appendix B3-Design Results for Mixed Conducting Ceramic Oxide Membranes.....	83
Appendix C-Calculations for Determining the Cold Face Temperature of the Vacuum Insulation Panels	84
Appendix D-Double Pipe Heat Exchanger Design.....	85
Appendix E-Cryogenic Oxygen Separation.....	87
E.1 Introduction and Theory.....	87
E.2 Structured Distillation Column	89
E.3 Series of Flash Tanks vs. Distillation Column.....	90
E.4 Modified Oxygen Generation Process	91
E.5 Cost Evaluation	93
E.6 Cryogenic Technology Summary.....	93
Appendix F- NPW, TCI Calculations and Happiness Graphs.....	94

List of Figures and Tables

Figure 1: Nasal Cannula.....	5
Figure 2: <i>Life Style Portable Oxygen Concentrator</i>	10
Figure 3: Typical Membrane Forms (a) flatsheet, (b) spiral-wound, (c) tubular, (d) hollow fiber. ¹⁸	13
Figure 4: Ionic Ceramic Oxide Membrane Operating Principle.....	14
Figure 5: Portable Oxygen Device Schematic.....	17
Figure 6: Detailed membrane stack schematic	19
Figure 7: Membrane Stack Drawing ⁴⁰	19
Figure 8: Sealant Bond Strength vs. Temperature ³⁶	23
Figure 9: Heat Exchanger 1-Oxygen and Air	26
Figure 10: Heat Exchanger 2-Nitrogen and Air.....	27
Figure 11: Effect of Pressure Rise on Thermal Conductivity ³⁸	32
Figure 12: Flow Diagram for Air Separation PSA System ⁵¹	37
Figure 13: Pressure Histories of Columns and Storage Tank in PSA Device.	38
Figure 14: Langmuir Equilibrium Adsorption Isotherms for Argon and Oxygen ⁶⁵	41
Figure 15: Fractional Uptake Versus Time for Oxygen and Argon on Bergbau-Forschung Carbon Molecular Sieve ⁶⁶	43
Figure 16: Steps of Oxygen Adsorbing PSA Cycle. ⁶⁶	44
Figure 17: E Size Oxygen Cylinder ⁶⁸ Which Provides 205 Minutes of Oxygen at 5 L/min.....	46
Figure 18: Pressure Swing Adsorption Process Flow Diagram.....	52
Figure 19: Effect of Advertising on the Alpha Function	53
Figure 20: Beta Function vs. Time for Various Happiness Ratios	55
Table 1: Parameters and Values for BICUVOX Ionic Ceramic Membrane Calculations ¹⁸	
Table 2: Heating Element Parameters and Calculated Values.....	21
Table 3: Thermal Conductivity Comparison	31
Table 4: BICUVOX Membrane Prototype Device Costs	36
Table 5: Adsorbent Data for Oxysiv 5 ⁹	39
Table 6: Itemized Cost of Components of Bottling Device.....	50
Table 7: Weights of Individual Components of Bottling Device	51
Table 8: Happiness Values for 95 % Oxygen Concentrator	56
Table 9: Consumer Happiness for 99% Oxygen Bottle Refiller vs. Delivered Oxygen..	56
Table 10: Consumer Happiness for Membrane Concentrator vs. AirSep Lifestyle	57
Table 11: TCI Calculation for Membrane Device	58

1.0 Executive Summary

A portable device that generates oxygen from air was designed and priced. The device produces a 5 liter per minute steady stream of 99.9% pure oxygen to individual patients. The device uses ceramic oxide membrane technology using BICUVOX membranes and is operated using a 12 V DC battery lasting 4 hours with 2 hours recharge time. The device is rectangular (16 in x 15.5 in x 13.9 in) weighing approximately 18 pounds. The cost estimate for the device is approximately \$2500.

An alternative pressure swing adsorption device was also designed. The device can produce 5 liters per minute of 99% oxygen which can be used to fill portable oxygen canisters. The cost for building the device is estimated to be \$4200. The device is about the size of a standard kitchen refrigerator and consumes approximately \$75 of electricity per month. Polymer and cryogenic technologies were also considered.

An economic analysis of the designed devices was performed. The selling price for the pressure swing tank re-filler is \$18,500 with a total capital investment of \$80 million and a net present worth of \$105 million. For the membrane portable oxygen generator, the selling price is \$11,000, the total capital investment is \$133 million, and the net present worth is \$166 million dollars.

2.0 Design Motivation

2.1 Introduction to Oxygen Therapy

2.1.1 Oxygen Therapy Use

People of all ages can be prescribed by a doctor to use an oxygen therapy device. As of April 1998, there are more than 800,000 oxygen therapy patients in the United States alone¹. Most oxygen therapy patients have been diagnosed with a disorder called hypoxemia, in which the lungs are incapable of providing enough oxygen to the bloodstream. Hypoxemia may be caused by a number of conditions such as asthma, chronic bronchitis, anemia, pulmonary edema, and congestive heart failure².

Oxygen therapy, in which the patient directly inhales oxygen through either a mask or nasal cannula, is an effective method for treating hypoxemia. A nasal cannula is the most common application method in which the patient inhales the oxygen by inserting short plastic tubes into the nostrils. These short tubing pieces are connected to a longer, thin piece of plastic tubing which runs to the device. A picture of a nasal cannula can be seen in the figure below³.



Figure 1: Nasal Cannula

Cannulas are used with various types of devices that can provide oxygen to the patient, including compressed oxygen tanks, liquid oxygen tanks, and oxygen concentrators. Oxygen is considered to be a prescription drug by the medical community

because it is administered at close to 100% purity¹. Therefore, one must have been prescribed to use oxygen therapy by a medical professional in order to purchase one of these oxygen devices.

The majority of oxygen therapy patients are elderly or disabled people. However, people of all ages, including small children, can be prescribed to use oxygen therapy depending on their medical condition. The way the oxygen is administered usually depends on the patient's age and condition. Most adults and older children use a nasal cannula, while younger children may be required to use an oxygen mask or tent to ensure sufficient administration of oxygen. When prescribing oxygen therapy, doctors specify a particular flow rate and concentration needed by the patient. Flow rates ranging from 0.5-8 L/min can be prescribed depending on the severity of the patient's condition. The average oxygen flow rate prescribed to most patients is 2 L/min⁴. The doctor usually suggests the type of oxygen therapy unit to be used by the patient. However, the choice may depend on insurance coverage and availability.

2.1.2 Medical Insurance Coverage

Oxygen therapy can become an expensive treatment over time. The cost of equipment, maintenance, tanks, and doctor visits can become quite substantial. The average cost of receiving home oxygen therapy ranges from \$300-\$500 per month². However, most private insurance companies, HMOs, and Medicare do include oxygen therapy coverage for people who have been officially prescribed by a physician.

Most private insurance companies provide at least partial coverage for oxygen therapy related expenses. Most health maintenance organizations, or HMOs, cover 100% of the oxygen therapy expenses, assuming all criteria are met. HMOs usually offer fewer choices when it comes to choosing a doctor, location, or type of treatment in exchange for lower monthly insurance costs⁵.

Medicare covers oxygen therapy expenses for patients who qualify and are over 65 years of age. Coverage may differ from state to state. In Oklahoma, Medicare covers 80% of all oxygen therapy related expenses, whether or not the equipment is rented or owned. This coverage includes the oxygen contents, supplies, equipment, and delivery of supplies. Portable oxygen systems, such as a generator, are not covered if only used as a

supplement to a stationary system at home. As an example, for a patient prescribed to only use oxygen while sleeping, a portable device would not be covered by Medicare. However, if the portable device is the primary source of oxygen, coverage will be provided. In order for the remaining 20% of costs of oxygen therapy to be covered, the patient must subscribe to Part B Medicare for which an annual \$110 deductible must be paid before Medicare pays the remaining portion of the therapy costs⁶. If the oxygen has been prescribed by a physician and deemed medically necessary, the expenses will most likely be covered. However, coverage does depend on the individual's actual plan. Therefore, the patient must always check with their provider before therapy begins to ensure they are covered.

2.2 Existing Oxygen Therapy Devices

There are currently numerous oxygen therapy devices available on the market. The three most common device categories are compressed oxygen tanks, liquid oxygen tanks, and oxygen concentrators. Currently, the most common type of device used by patients is the compressed oxygen tank. However, all three technologies are used frequently and possess their respective advantages and disadvantages.

2.2.1 Compressed Oxygen Tanks

Compressed oxygen comes in gaseous form in tanks which are delivered to the patient on a weekly or monthly basis. A flow meter and a regulator are attached to the tank so that the user can easily adjust the oxygen flow to their prescribed flow rate. Tanks are available in various sizes, including large stationary tanks to be used in the home and small portable tanks for use away from home. Compressed oxygen is usually not prescribed for severe cases of hypoxemia. Most compressed oxygen users only need the oxygen supplement occasionally, such as when exercising or performing any physical activity.

Compressed oxygen tanks have many advantages. They are small, lightweight, and do not require any electricity. Most oxygen tanks can be pulled by a small, lightweight cart with wheels to increase mobility. Several tanks can be used to extend

portability time away from home. However, this requires transport of the extra tanks, which can be a burden on the patient.

High oxygen flow rates greater than 5 L/min can also be achieved using compressed oxygen tanks by simply adjusting the flow meter. Physicians are also likely to prescribe a compressed oxygen system to those patients that require oxygen of high purity, since the oxygen is delivered as a high purity gas. Another significant advantage of compressed oxygen is that the contents of the tank will not evaporate over time, as they can in liquid oxygen tanks⁷.

Compressed oxygen tanks do possess a few key disadvantages for users. The most significant disadvantage is the fact that the tanks will eventually run out of oxygen, causing the need for delivery of new tanks. Compressed oxygen is also stored in the tanks at very high pressures which can be very hazardous if dropped. Patients must take extreme care not to expose the tanks to high heat, flame, or accidentally drop them.

2.2.2 Liquid Oxygen Tanks

Oxygen is stored in tanks as a liquid at very low temperatures in this type of oxygen system. Most liquid oxygen systems have a large stationary unit that stays at home, as well as a smaller, portable unit that can be filled by the user when leaving the home. This is one of the advantages of using liquid oxygen as your primary oxygen source. The smaller, portable tank only weighs approximately 5-13 lbs. Upon receiving the liquid oxygen system, the user is instructed on how to fill the small tank properly by a professional. Just like compressed oxygen systems, the liquid oxygen systems do not require electricity, can achieve high flow rates and high oxygen purity, and are also very quiet.

Even though more oxygen can be stored in liquid form than in gaseous form, the liquid oxygen tanks will empty out eventually. A technician must visit the patient's home regularly to refill the stationary liquid oxygen tank. This can be a nuisance to the user and is a major disadvantage. Also, liquid oxygen will evaporate over time, whether or not the tank is in use. Therefore, a patient might end up paying for extra oxygen to be delivered if they run out sooner than expected due to evaporation.

2.2.3 Oxygen Concentrators

Oxygen concentrators, sometimes called generators, are electric oxygen systems that generate their own oxygen. They do this by extracting oxygen from the air and delivering it to the patient, while discharging the nitrogen-rich air stream back into the environment. Therefore, concentrators provide an unlimited supply of oxygen and there is no need for delivery or refilling of tanks. The unlimited supply of oxygen is perhaps the biggest advantage of owning a concentrator. In addition, concentrators will require minimal maintenance after installation, as opposed to large stationary tanks which need to be maintained regularly due to their hazardous nature.

The oxygen concentrators that are currently on the market have many disadvantages. Most are not portable and are very large, weighing over 50 lbs. Generators can consume as much as 250-400W of power, depending on the size and oxygen flow rate. Concentrators require electric motors that can create noise, as well as increase the patient's electric bill. The electric bill increase would be equivalent to that of running a small, color television set continuously in the home⁴.

Since the concentrator has an electric motor, there is a need to have a backup supply of oxygen on hand in case of a power outage. Most concentrators can only achieve oxygen flow rates of less than 5 L/min, and the purity of oxygen obtained is limited to 90-95%. Oxygen concentrators can also be much more expensive to purchase than tanks, costing from \$2000-\$5000. However, this is a one-time expense when purchasing the device. To continue therapy with compressed oxygen or liquid oxygen tanks, the patient must continue to pay for tank delivery, refills, and tank maintenance⁸.

There are a limited number of portable oxygen generators on the market today. One in particular is the *LifeStyle Portable Oxygen Concentrator* from the AirSep Corporation. This device uses a molecular sieve technology combined with an oxygen conserving technology which only delivers oxygen to the user during inhalation. The unit detects inhalation and delivers a flow of oxygen equivalent to the designated flow rate required by the user. This conservation of oxygen results in the need for a smaller device, enabling the unit to become portable. A picture of the device is shown in the figure below⁹.



Figure 2: *Life Style Portable Oxygen Concentrator*

The device is small with dimensions of 5.5x 7.25x 16.31 inches and weighs only 9.75 lbs. The concentrator consumes 42 Watts and can be run off of DC, AC, and battery power. Equivalent flow rates ranging from 1-5 L/min can be achieved using this device. However, the attainable oxygen purity levels are low, ranging from only 87-93%. The *LifeStyle* is relatively quiet but produces too much noise to be used in quiet settings, such as church. The device is also very expensive, costing the patient approximately \$5,000. This price does not include any accessories such as a roll-cart, which sells at a price of \$195 on the AirSep website.

Perhaps the biggest downfall of the *LifeSyle* concentrator is the battery life. The total battery life is only approximately 50 minutes. The battery recharges for 2-2.5 hours while the device runs on AC power. This does not offer the patient much mobility time. To compensate for the short battery life, many users must buy additional batteries to use with a *PowerPact Battery Charger* device, sold separately at a cost of \$295. This does not include the price of the additional batteries, which can cost the patient about \$100 each.

Current portable oxygen concentrators have many disadvantages, including low battery life, low oxygen purity, high noise, and a high price tag. There is a need for the development of a more efficient and reliable portable device that can be purchased at a reasonable price. A quieter, less expensive device with high oxygen purity, flow rate, and battery life capabilities would be extremely advantageous to all oxygen therapy users. To achieve these desired properties, membrane gas separation and pressure swing adsorption technologies were investigated to develop an improved portable oxygen concentrator device.

3.0 Membrane Gas Separation Technology

3.1 Introduction to Membranes

Membranes are semi-permeable barriers which can be used to separate multiple component feed streams into product streams of higher purity. The separation process occurs due to the difference in the abilities of the components to pass through the membrane. The portion of the feed stream which passes through the membrane is called the permeate stream, and it has a higher concentration of the faster components than the feed stream. The remaining portion of the feed that does not pass through the membrane is called the nonpermeate or retentate stream. The concentration of the slower components in the retentate is higher than that in the feed stream¹⁸.

The general equation for flux of component i through a membrane is given by

$$N_i = \frac{P_i}{l} (\text{driving force}) \quad (1)$$

where P_i is the permeability of component i through the membrane material, l is the thickness of the membrane, and the final term represents the driving force required to induce the flux. There are a variety of driving forces which apply to different membrane applications and materials.

Membranes can be used for a number of separation applications including reverse osmosis, dialysis, microfiltration, and gas permeation. The membrane application of

interest for this study is gas permeation with the objective of separating air into oxygen- and nitrogen-enriched streams. Polymers and ceramic oxides are the material types investigated in this project. Polymer membranes are considered because they are widely used industrially to produce high purity nitrogen streams from air²³. Ceramic oxide membranes are of interest because modification of the solid oxide fuel cell process to exclude the reaction of the oxygen permeate with a fuel stream can be used to produce a high purity oxygen stream at high temperatures¹⁹. Ceramic oxides can be divided into two categories based on their ability to transport ions and electrons. The ionic subcategory can transport ions while the mixed conducting subcategory is capable of conducting ions as well as electrons.

Membranes are typically fabricated in flat sheet, spiral-wound, tubular, or hollow fiber forms. Flat sheets are plates or disks with planar surfaces which can be operated alone or arranged in a stack. Spiral-wound membranes are essentially elongated thin flat sheets which are wrapped tightly around an axial collection tube with space allowed between the sheets for flow. Tubular designs consist of several (usually 30 or fewer) hollow tubes with typical diameters from 0.5 to 5 cm. Feed flows through the tubes, and permeate is collected in an outer tube that surrounds all the smaller tubes. Hollow fiber membranes modules have a number of small hollow tubes with outer diameters on the order of 10 to 100 μm bundled together and arranged parallel to one another. A larger tube surrounds the entire bundle. Figure 3 shows sketches of these typical membrane forms. Each of these designs can have a variety of different flow arrangements regarding the specific sides of the membrane that each stream flow past and the direction of the two streams relative to one another^{24, 25}.

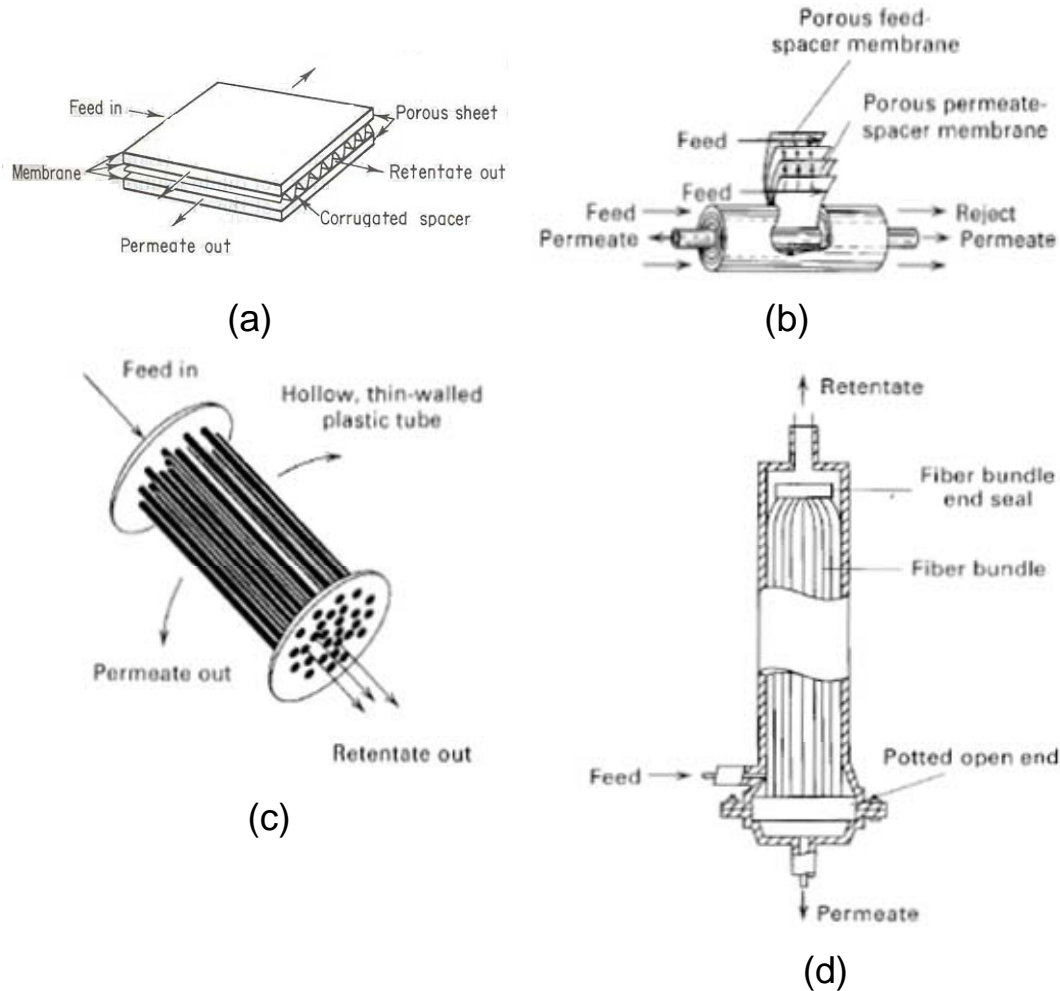


Figure 3: Typical Membrane Forms (a) flatsheet, (b) spiral-wound, (c) tubular, (d) hollow fiber.¹⁸

3.2 Ionic Ceramic Oxide Membranes

3.2.1 Principles

Ionic ceramic oxide membranes operate while being electrically driven by an external voltage source. Like mixed conducting ceramic oxides, they operate at high temperatures and only allow oxygen flux through the membrane. Because the driving force is independent of the pressure, these membranes can operate without requiring pressurized feed. Figure 4 is a schematic of how ionic ceramic oxide membranes function.

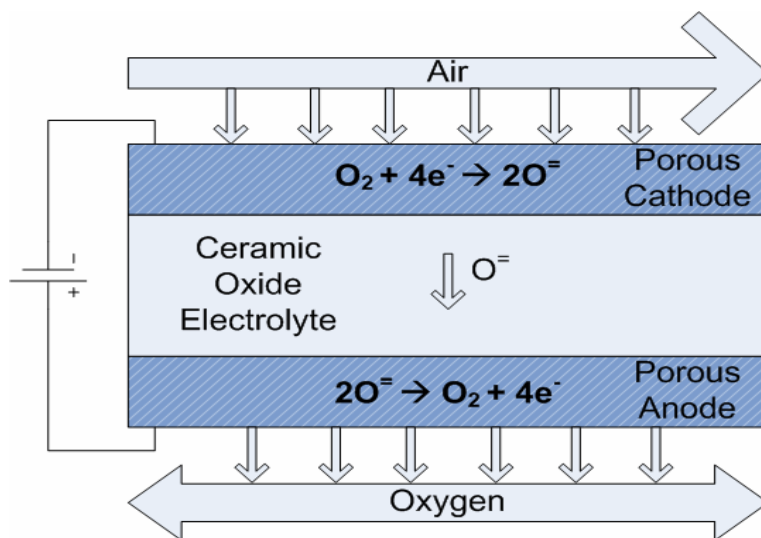


Figure 4: Ionic Ceramic Oxide Membrane Operating Principle

3.2.2 Materials

Oxides with fluorite-related structures such as yttria-stabilized zirconia (YSZ) and doped ceria, oxygen-deficient perovskites, and BIMEVOX ceramics are common ionic conducting ceramic materials used for this type of application²⁶. BIMEVOX ceramics are bismuth vanadates with metals such as zinc, copper, and cobalt substituted for portions of the vanadium. YSZ is the most commonly used ionic conducting membrane material. The range of temperature operation for YSZ is 800-1000°C. BIMEVOX varieties give oxygen flux similar to YSZ while the operating range is 400-600°C. The lower temperature operation is favored because it reduces the requirements for heating the cells, cooling the exhaust streams, and insulating the apparatus.

Boivin, et al³² studied the performance of different BIMEVOX electrolytes—BICUVOX, BICOVOX, and BIZNVOX. They found that all three electrolytes exhibit current densities up to 1 A/cm² and operate at high Faradic efficiency which is related to the recovery of oxygen from the feed. Xia, et al³³ report that BICUVOX.10 (Bi₂V_{0.9}Cu_{0.1}O_{5.35}) ionic conductivities are 50-100 times higher than other solid electrolytes. Based on those findings, BICUVOX.10 is chosen as the electrolyte material.

3.2.3 Modeling of Membrane Performance

The literature typically gives experimental results for BICUVOX rather than modeling equations based on the mechanism of oxygen transport. In this study the electrochemistry equations are used to design the membrane. The user first specifies the

desired volumetric flow rate of oxygen to be transported across the ionic ceramic oxide membrane. In addition, the number of membrane plates and their thickness should be specified. Then the Faraday relationship is used to determine the current requirement, I_M ,

$$I_M = \frac{4QF}{n} \quad (2)$$

where 4 is the number moles of electrons required to dissociate 1 mole of oxygen molecules, Q is the molar flow rate of the oxygen permeate, F is the Faraday constant, 96485 C/mol electrons, and n is the number of membrane sheets.

The total area required for the separation is based on the current density of the membrane material. BICUVOX.10 at 585°C has a current density of approximately 0.75 cm²/A.³² The current found by equation 2 is multiplied by the current density to determine the membrane area required. The total membrane area is divided by the number of sheets, giving the area of each sheet. For convenience, the model equations assume that each sheet is square.

The voltage drop across each membrane, E , is calculated using the Nernst potential,

$$E = \frac{RT}{zF} \ln \frac{y_{O_2,h}}{y_{O_2,l}} \quad (3)$$

where R is the ideal gas constant, T is the operating temperature, z is the number of electrons required per ion, F is the Faraday constant, y_{O_2} is the concentration of oxygen, and the subscripts h and l refer to the high and low concentration sides of the membrane.

4.0 Ionic Ceramic Membrane Design Results

The goal of the present study is to design a portable device that can produce high purity oxygen from air using membranes. Ideally, the device would have dimensions of approximately 12 in x 7 in x 7 in, be lightweight, and operate with battery power. In

addition to these considerations, the device should be capable of producing a 5 lpm product stream with greater than 93% purity of oxygen.

Based on design size consideration, BICUVOX plates were specified as 2.4 in. wide by 2.4 in. long with thickness of 0.38 cm. Between the plates, air channels exist for the feed/retentate streams and the permeate streams. The air channel height was set as 0.75 cm in height. Electrodes separate the air channels between each plate. The thickness of the electrode between two air channels was set to 0.2 cm.

Because of the parallel flow arrangement of the feed and permeate streams in each cell in the stack, the feed stream is divided equally between the 48 cells in the cell stack. The 48 cells are arranged in 4 cell stacks with 12 cells in each stack. Assuming a density of 5.75 g/cm^3 , the total mass of the 48 ceramic cells is 8.6 lb.⁴² The estimated density was based on the density of a different ceramic that is also used for oxygen membrane separation. This arrangement was chosen to reduce the amperage required to operate the membrane cell stack and to offer a more portable configuration. The current required for oxygen flow rate of 5 lpm through 48 cells, 2.4 in. wide and 2.4 in. long, is 28 A. The current density is the ratio of the current divided by the cell cross sectional area. The current density is 0.75 A/cm^2 which is a valid value for BICUVOX.10. The electrodes are connected in series to minimize the current required to power the cell stack. The voltage drop is 0.057 V/cell and the total voltage drop across the cell stacks is 2.75V.

5.0 Description of Device Components

The flow of air through the device begins as ambient air is drawn into the oxygen concentrator device by two rotary compressors. The air is then passed through a heat exchanger where the ambient stream cools the hot oxygen and nitrogen gas streams leaving the membrane cell stack. The warmed feed air is then directed into the membrane stack. In the stack, the air stream is heated to 585°C and separated into two streams: a pure oxygen stream and a nitrogen-rich stream. These hot streams exit the membrane stack and pass back through the heat exchanger to reject heat to the cold incoming ambient air. The cooled nitrogen-rich stream exits the heat exchanger and is exhausted from the unit at 41°C . The cooled oxygen stream also exits the heat exchanger

at 41°C and flows through the cannula which supplies the oxygen stream to the user. A schematic of the entire device is seen in Figure 5. The total volume is 2 cubic feet.

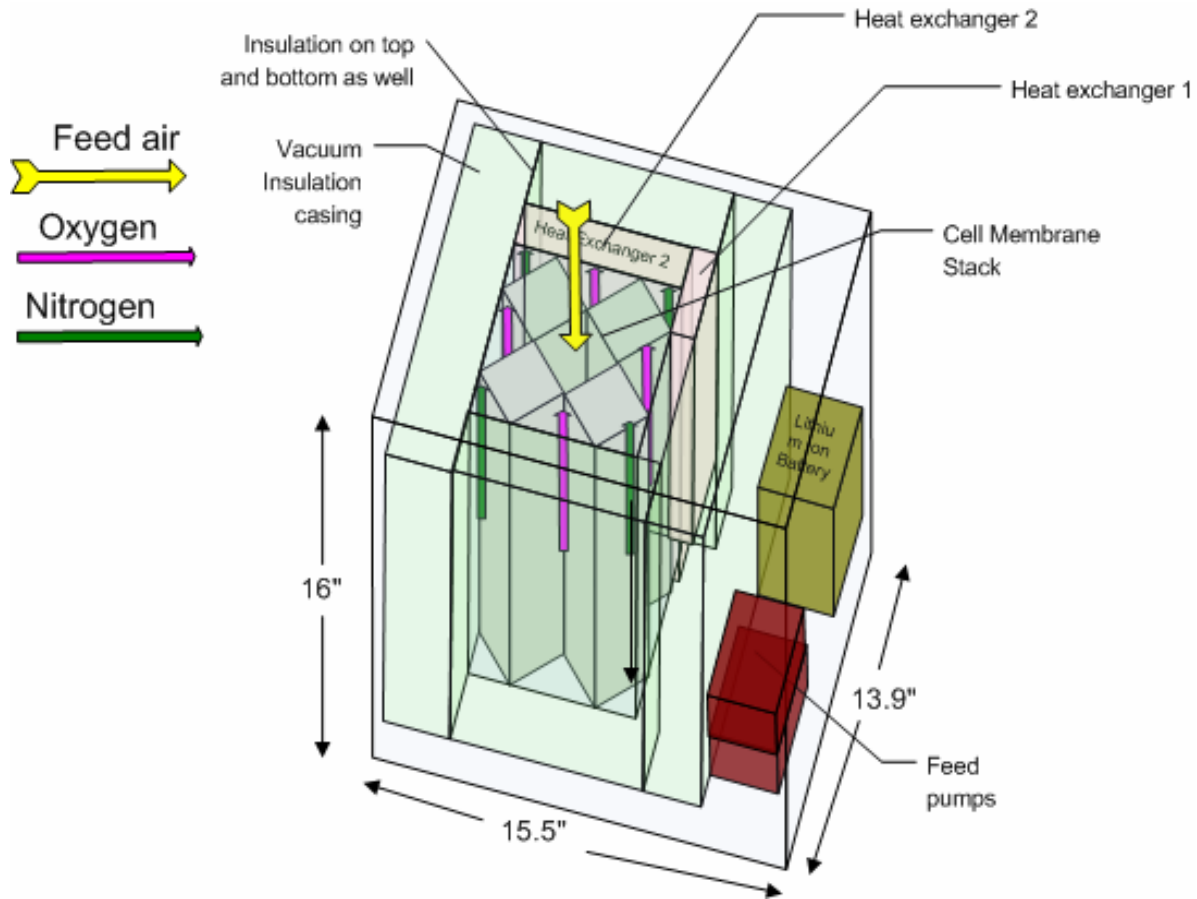


Figure 5: Portable Oxygen Device Schematic

5.1 Membrane Stack

The membrane stack is a series of 48 2.4" x 2.4" BICUVOX.10 ceramic membrane plates 0.38 cm thick sandwiched between layers of Inconel electrode plates. The voltage drop across the 10" tall stack is 2.75 V with a current of 28 A. Table 1 summarizes the specified and calculated parameters for the membrane stack.

Table 1: Parameters and Values for BICUVOX Ionic Ceramic Membrane Calculations

Parameter	Value	
number of plates	48	plates
Temperature	585	C
total volumetric flow rate of permeate	5	L/min
molar gas volume (STP)	24.04	L/mol
molar flow rate of permeate/plate	0.00007	mol/s/plate
electron stoichiometry	4	mol electrons/mol O ₂
Faraday constant	96485	C/mol electrons
current	27.868	A
current density for BICUVOX.10	0.75	A/cm ²
total plate area required	37	cm ²
side length of square plates	6.10	cm
thickness of plates	0.38	cm
air gap height	0.75	cm
electrode height	0.2	cm
total cell stack height	100.04	cm
number of columns	4	
height per column	9.85	in
volume of plates	41.36	in ³
density of ceramic	0.21	lb/in ³
mass of ceramic	8.60	lb
electrical potential for each cell	0.057	V
total potential for stack	2.751	V
power required	76.675	W
oxygen recovery from feed	0.80	
feed flow rate	30	L/min

The feed air to the ceramic membranes, assumed to be 21% oxygen and 79% nitrogen, flows into the ceramic cell stack through one flow channel and is split to flow simultaneously through each channel above each of the BICUVOX plates. After a surface reaction converting O₂ to 2O⁻², the oxygen ions flow through the BICUVOX plates and react to form O₂ at the bottom face of the BICUVOX plate. As the pressure of oxygen builds up on the pure oxygen, product side, it flows out of the cell stack to a heat exchanger to be cooled. The feed air rich in nitrogen that passes over the ceramic plates combines into one flow and exits the stack to the heat exchanger. Figure 6 shows a detailed diagram of the device with arrows denoting the direction of air flow.

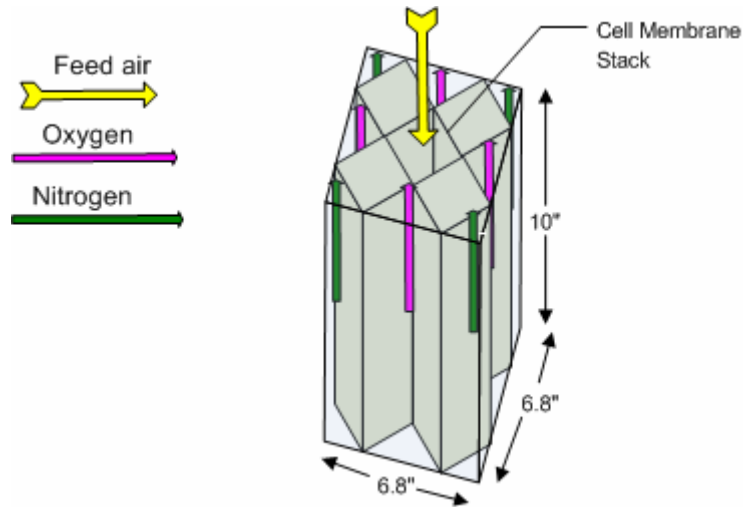


Figure 6: Detailed membrane stack schematic

Figure 7 shows the direction of air as it flows through the individual membrane cells in each stack.

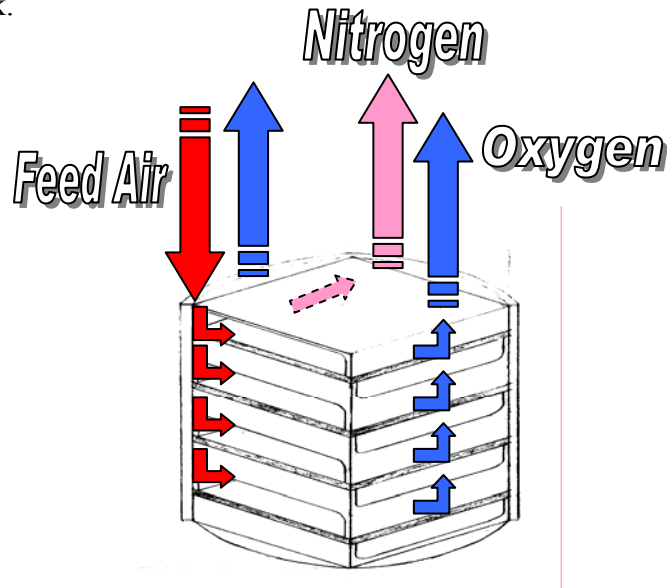


Figure 7: Membrane Stack Drawing ⁴⁰

Inconel was chosen for the electrodes for its high temperature and corrosion resistant qualities. It has an electrical resistivity of 103 mΩ-cm, a melting point of 1370°C, a density of 8.25g/cm³, and a coefficient of expansion of 11.5 at 20°C. It is a metal alloy consisting of 76wt% Ni, 17wt% Cr, and 7wt% Iron.

Three high resistance wires are arranged in the air feed stream to heat the ceramic cell stack through. The 24 gauge wires are attached at the top of the air entry space and extend 4.80 in. into the cell stack. The wires are electrically in series to decrease the amperage requirement. The 4.80 in. wires use radiative heat transfer to heat the stack and convective heat transfer to heat the incoming air. The wires will heat the ceramic cell stack to 585°C after a 20 minute startup time and will maintain 585°C for continuous operation. High temperature sealant is used to seal the corners of the square ceramic plates and Inconel electrodes to the cell stack housing to maintain gas separation between the feed air, nitrogen rich exit stream, and oxygen rich streams. The sealant will also be used to bond each Inconel electrode to the ceramic plate above and/or below it in the stack.

A housing of magnesium oxide encapsulates the ceramic membrane/Inconel cell stack. Magnesium oxide is able to withstand high temperatures, up to 2800°C, has good thermal and electrical resistivity; specific resistivity of 10^{17} Ω -cm. MgO also has thermal expansion properties similar to the Inconel and BICVOX materials with a thermal expansion coefficient of 8.0×10^{-6} K^{-1} . This property is essential to maintain the seals between gas flow streams inside the cell stack. To protect the components inside the oxygen concentrator unit from the high temperatures inside the ceramic stack, vacuum panels are placed around the magnesium oxide housing. The vacuum panels are 6.5cm thick and give a cold face temperature of less than 27°C at the outside face of the vacuum insulation panel.

5.2 Heating Element

In order to start up the device, the membrane stack must be heated to the operating temperature. Once the system reaches steady state, the temperature of the cells is maintained by the preheated feed stream. Nichrome-60 (Ni Cr C) wire resistors are used to transfer heat to the system during start up. The three resistors are located in the center air feed stream between the four membrane stacks. Material specific parameters such as current/length of wire required to heat the stack to the operating temperature and the resistance/length were used to calculate the power needed to operate the heating element. The cost of the wires of the heating element is approximately \$5 if they can be

purchased in bulk at a rate of \$0.80 per foot. The weight of the wires is 0.70 lb. A twenty minute start up time was assumed, and the total power needed for the heating element while in use is calculated as 66 W. Table 2 shows the listing of the parameters and calculated values for the heating element^{27,28}.

Table 2: Heating Element Parameters and Calculated Values

wire design: 3 vertical wires along the feed stream		
wire length/air entry point	4.80	in
current/length of wire to heat wires to 585 C	4.58	A/ft
current for 3 parallel sets of resistors in parallel, I_H	5.50	A
resistance/length of wire	1.82	ohm
resistance of each wire	0.7276	ohm
price/length of wire	0.80	\$/ft
price of wires	0.96	\$
weight/volume of wire	0.30	lb/in ³
diameter of 24 gauge wire	0.20	in
total weight of wires	0.36	lb
equivalent resistance of 3 wires in parallel, R_H	2.18	ohm
assume start up time	20	min

5.3 Sealant

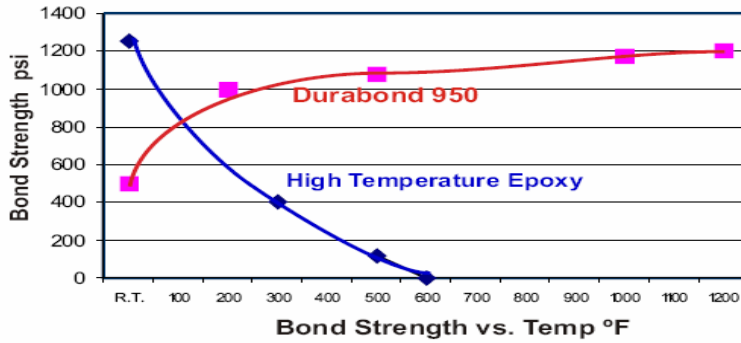
Sealants were required in the ceramic electrolyte stack to maintain separation of gas streams. Without proper sealing the feed airflow would be allowed to flow into the pure oxygen product stream, greatly reducing its purity. Several criteria were established to in order to select the best sealant. One consideration was the ability of the sealant to withstand the operating temperatures up to 600°C inside the electrolyte cell without breaking down. The sealant must also have a bond strength required to maintain its seal as the membrane stack thermally expanded.

Another consideration was the health hazards associated with any vapors given off by the sealant. The location of the sealant in the electrolyte cell meant that any vapors given off would be inhaled by the individual using the oxygen concentrator unit. Based on this concern, any sealant that produced even minor health effects should not be used in the construction of the membrane stack. The Material Safety Data Sheets (MSDS) for each sealant were examined to ensure consumer safety.^{37,72} The design of the electrolyte

cell required that an electric current run through the ceramic oxide membrane and the Inconel plates separating the ceramic membranes. This meant that the sealant must be an electrical insulator since it is used between the Inconel and ceramic membrane, and the cell housing.

Based on the criteria established to select a sealant, none were found to have all the desired properties for use in the oxygen concentrator unit. The two sealants that most closely fit the established criteria were Resbond™ 907GF and Durabond™ 950, both manufactured by the Cotronics Corp³⁶. Resbond™ 907GF has a usable temperature range of 300 – 2350°F, with a maximum rated temperature of 3000°F and a continuous service temperature of 2350°F. Subject to temperatures inside its usable range produce an elongation of 5% which exactly matches the thermal expansion properties of the membrane stack and the housing material. This property greatly reduces the possibility of internal gas leakage, since the sealant expands with the materials it is bonding, and makes Resbond™ an attractive sealant for this device. Another desired property of Resbond™ is its dielectric quality. It has a Dielectric constant, at 10⁸ cps, of 3.0, and a volume resistivity of 10⁹ ohm-cm.

Although Resbond™ has many qualities that make it ideal for use in the oxygen concentrator, it is undesirable due to its possible health effects. The MSDS for Resbond™ states that the sealant contains refractory ceramic fibers, which are suspected carcinogens in laboratory animals. The effects of the ceramic fibers have not been thoroughly tested enough to determine their health effects on humans. The Thermal Insulation Manufacturers Association (TIMA) is currently sponsoring inhalation and epidemiological studies on industry workers exposed to the ceramic fibers. Until studies are completed that show no health risks, the Resbond™ sealant cannot be used. The sealant also contains minor amounts of organic binders which burn out during first heat up, and can cause respiratory irritation if inhaled. Durabond™ 950 also had some desirable qualities. It may be used up to 1200°F, and its bond strength increases with increased temperature. At 1200°F, its bond strength is 1000psi, at 200°F it is 500psi. Figure 8 shows the bond strength of the sealant vs. temperature.



This graph compares the bond strength of Durabond 950 with a typical High Temperature Epoxy. Note the epoxy weakens with temperature and the Durabond 950 increases in strength with temperature.

Figure 8: Sealant Bond Strength vs. Temperature³⁶

Like the Resbond™ sealant, Durabond™ has health concerns associated with it that exclude it for use in the oxygen concentrator design. The International Agency for Research on Cancer shows inadequate evidence that metallic nickel or chromium contained in the Durabond™ sealant is carcinogenic to humans, but has been shown to be carcinogenic to animals. Due to the unknown negative effects on humans, this sealant cannot be used.

Many sealants exist that do not produce harmful vapors at low temperatures, however; these were not considered since they cannot withstand the operating temperatures of the ceramic cell. At high operating temperatures, these sealants will break down chemically and either release hazardous fumes, or produce cracks and gaps that would render the oxygen concentrator useless. To meet the special requirements of the oxygen concentrator design, a special sealant is required. No sealant currently on the market can meet all of the critical requirements necessary for a sealant used in this design. For this design to function safely, a new sealant combining the desired properties; the ability to withstand high temperatures, possessing the desired dielectric effect, and posing no health hazards, must be designed and tested. Another possibility is to use an existing sealant with a coating that would prevent harmful vapors or particles from escaping into the oxygen product stream.

5.4 Heat Exchanger

5.4.1 Heat Exchanger Background

Significant heat exchange is needed within the oxygen device due to the very high operating temperature of the cell membranes. The cell stack operates at approximately 600°C, so the exiting oxygen and nitrogen-rich streams are at very high temperatures. In addition, the feed air stream enters the device at room temperature and needs to be heated. Therefore, the heat from the hot oxygen and nitrogen streams can be used to preheat the incoming air, while the hot streams are cooled to safe exiting temperatures. Special care must be taken to ensure that the exiting oxygen stream is cooled to near room temperature since this stream will come in direct contact with the patient. It would also pose a hazard to the user to have the exiting nitrogen-rich stream leave the device at unsafe temperatures.

The first heat exchanger design considered was a traditional double-pipe configuration. Double-pipe Nusselt number correlations for laminar flow from Perry's Chemical Engineer's Handbook³⁵ were used to calculate the pipe length required to achieve the desired temperature difference for the three streams of interest. Details of these calculations can be found in Appendix D. The result consists of splitting the feed stream into two double-pipe coiled heat exchangers, one for the feed air and oxygen and the other for the feed and nitrogen streams.

As can be seen from the calculations, the required pipe lengths needed to achieve a large enough temperature difference result in very large coils. Just one coil alone is 9.6in. in diameter and 9.5in. tall. The combined coil weight is over 12 lbs, even using aluminum pipes. This double-pipe configuration does not present a realistic heat exchanger for use in a portable oxygen device. A much smaller heat exchanger design is needed. This led to the exploration and development of a microchannel heat exchanger for use in this particular application.

Microchannels greatly reduce the size requirement of traditional heat exchangers by allowing much more heat exchange to occur within a compact area. As with any heat exchanger, an increase in available surface area results in more efficient heat exchange³⁴. Microchannel heat exchangers have significantly larger heat transfer surface areas than traditional heat exchangers because they contain small grooves, or channels, within the

exchanger. When gases flow through the channels, heat is more effectively transferred through the exchanger to the opposing side. The compact size of microchannel heat exchangers makes them very appealing in many small-scale processes, such as the generation of oxygen from a portable device.

5.4.2 Heat Exchanger Design

In order for the feed air stream to effectively cool the exiting oxygen and nitrogen streams, the feed is split into two streams. On the basis of a 30L/min feed, the first feed stream has a volumetric flow rate of 5L/min and cools the exiting 5L/min oxygen stream. The second feed stream has a flow rate of 25L/min and cools the 25L/min exiting flow of nitrogen. This arrangement calls for two heat exchangers, each with two streams of equivalent volumetric flow rates. The entry and exit temperatures for both the oxygen and nitrogen streams are 600⁰C and 41⁰C, respectively. Even though the oxygen will exit at 41⁰C, the stream will cool down significantly more while traveling through the nasal cannula to the patient. The entry temperature for the feed air is ambient at 21⁰C, and the exit temperature of the feed to the membrane is 580⁰C.

The first heat exchanger contains the 5L/min oxygen and feed air streams flowing counter-currently. This microchannel heat exchanger has dimensions of 1 in. x 3.4 in. x 7.9 in. with a mass of only 0.15 lbs. It is constructed from copper because of the high thermal conductivity of the material (350 W/m K) and contains 10 channels per stream, for a total of 20 channels. Each channel is 0.4 in. high, 0.31 in. wide, and 7.9 in. long. The outer wall thickness is 2.5mm, and the thickness of the layer in between the top and bottom channels is only 0.5mm. This very small thickness allows one to neglect the thermal resistance between streams, so heat is easily transferred between the two streams. The outer walls are also insulated to ensure negligible heat loss. The pressure drops are essentially negligible for both the oxygen and air sides, with values of only 3.6x10⁻⁴psi and 3.1x10⁻⁴psi, respectively. A schematic of the first heat exchanger can be seen in the following figure.

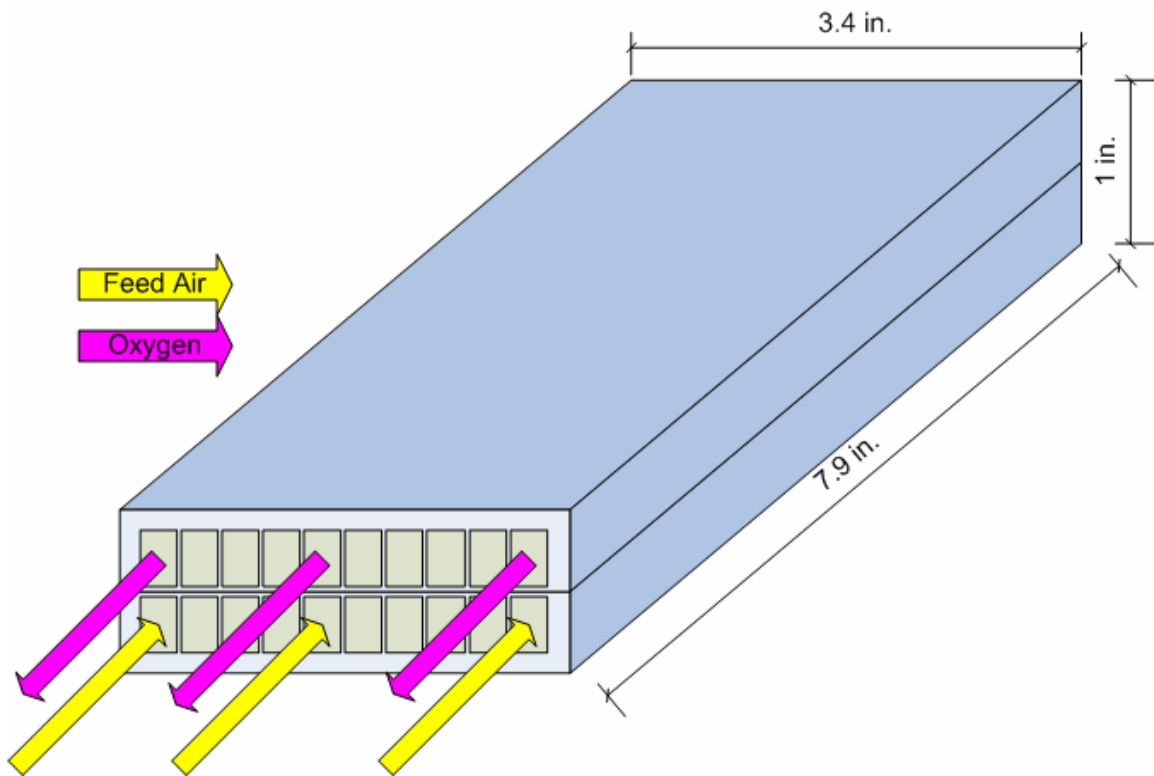


Figure 9: Heat Exchanger 1-Oxygen and Air

The second heat exchanger contains the 25L/min nitrogen and feed air streams, also flowing counter-currently. The microchannel heat exchanger has dimensions of 1.6 in. x 7.8 in. x 10 in. with a mass of 0.24 lbs. Together both exchangers have a total mass of only 0.39 lbs. This exchanger is also constructed from copper and contains 20 channels per stream, for a total of 40 channels. Each channel is 0.7 in. high, 0.37 in. wide, and 9.8 in. long. Just as before, the outer wall thickness is 2.5mm, and the thickness of the layer in between the top and bottom channels is 0.5mm. Insulation covers the outer walls as in the first exchanger. The pressure drops are again essentially negligible for both the nitrogen and air streams with values of only 0.000179psi and 0.000188psi, respectively. A schematic of the second heat exchanger can be seen below.

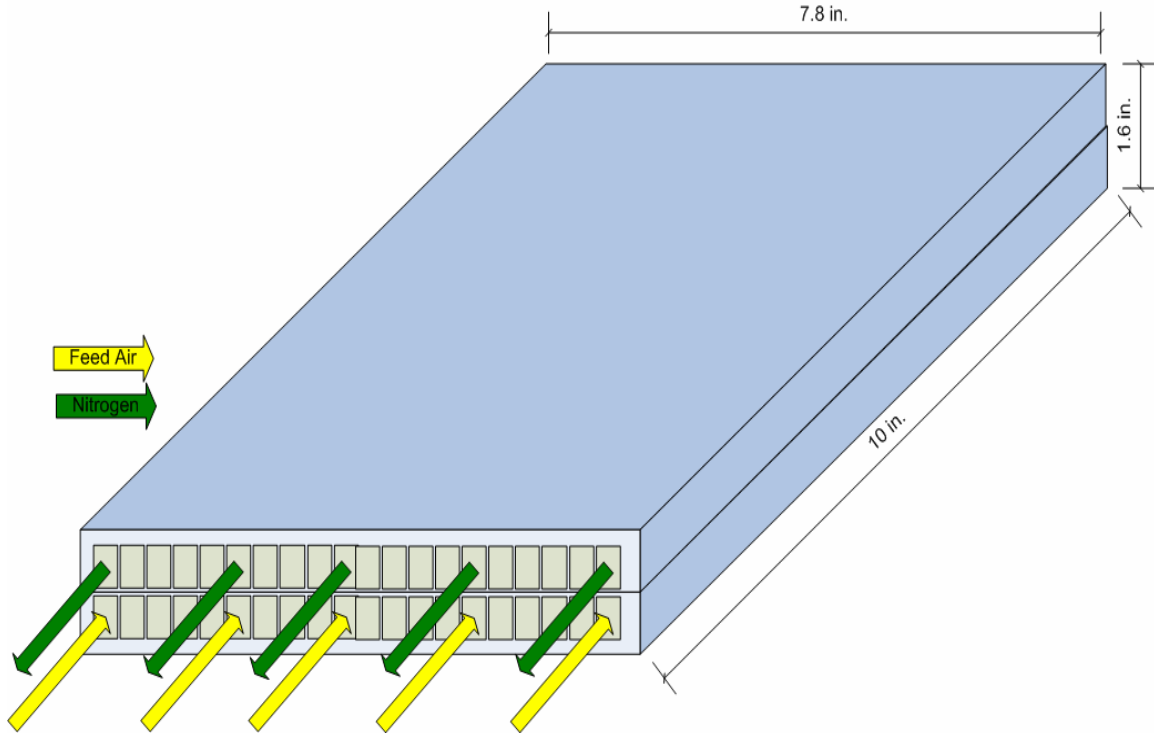


Figure 10: Heat Exchanger 2-Nitrogen and Air

In order to determine the heat exchanger dimensions, the necessary heat transfer area required to achieve the desired temperature difference was found using the overall heat transfer coefficient, U , found in the double-pipe calculations previously done. This value was then applied to each microchannel exchanger to find the heat transfer surface area, A , using the following equations:

$$\frac{1}{U} = \frac{1}{h_i} + \frac{r_o - r_i}{k} + \frac{1}{h_o} \quad (\text{From double-pipe calculation}) \quad (4)$$

$$Q = \dot{m} C_p \Delta T \quad (5)$$

$$Q = UA\Delta T_{LM} \quad (6)$$

where h is the convective heat transfer coefficient, r is radius, k is thermal conductivity of copper, Q is the heat transfer rate, \dot{m} is the mass flow rate, C_p is specific heat, ΔT_{LM} is the log-mean temperature difference, and subscripts i and o refer to the inner and outer pipe wall surfaces, respectively.

After solving for the area, the required surface area of each exchanger was found to be 0.11 ft^2 and 1.8 ft^2 , respectively. The dimensions of each microchannel exchanger

were then found by varying the length, height, and width of each channel, while simultaneously varying the number of channels in the device to achieve the required surface area. Outer wall thicknesses were set at 2.5 mm, and the middle layer thickness dividing the channels was set at 0.5 mm to ensure high heat transfer. The width in between each channel was also given a specified length of 0.18 mm. Simple surface area calculations were done (length times width) to find the heated surface area per channel, assuming that heat is only transferred on three sides of each channel (the two tall sides and either the top or bottom, depending on which stream is under consideration). The outer walls of the two end channels were also assumed not to conduct heat. Finally, the total heated surface area was found by multiplying by the total number of channels. The surface areas of exchangers 1 and 2 were found to be 0.56 ft² and 2.9 ft², respectively, which are sufficient for the heat transfer requirements.

The equivalent diameter of each channel was calculated and used to find the Reynolds number for each stream using the following equation.

$$\text{Re} = \frac{\rho D_{eq} v}{\mu} \quad (7)$$

where ρ is the density, v is the velocity, D_{eq} is the channel equivalent diameter, and μ is the viscosity. The Reynolds numbers for both streams in the oxygen-air exchanger were both around 19, which are very low and indicate laminar flow within the channels since the value is less than 2300. The Reynolds numbers for the nitrogen-air exchanger also indicated laminar flow with a value of 34. The velocities of each gas through the exchangers were found by dividing the volumetric flow rate by the sum of the cross-sectional areas of all the channels through which the gas flows. The velocities of the oxygen and the feed air in exchanger 1 were both 10.4 cm/s, while the velocities of the nitrogen and feed air in exchanger 2 were both 12.9 cm/s. The length of the exchanger divided by the velocity in each stream gave the retention time for each gas. Therefore, the oxygen and nitrogen streams can be successfully cooled down to 41⁰C in approximately 1.9 seconds of residence time in their respective heat exchangers.

Finally, the pressure drop in each exchanger was calculated using a pressure drop correlation for laminar flow in rectangular ducts found in Hesselgreaves⁴². The pressure drop equation is given as

$$\Delta P = \frac{4kLm^2}{2\text{Re}d_{eq}A_c^2\rho} \quad (8)$$

where L is the channel length, m is the mass flow rate, d_{eq} the equivalent diameter, and A_c is the cross sectional area. The term k is equal to the friction factor times the Reynolds number for rectangular ducts,

$$f\text{Re} = 24(1 - 1.3553\alpha + 1.9467\alpha^2 - 1.7012\alpha^3 + 0.9564\alpha^4 - 0.2537\alpha^5) \quad (9)$$

where

$$\alpha = \frac{\text{channel height}}{\text{channel width}} \quad (10)$$

The total pressure drops calculated for the oxygen and feed air channels in heat exchanger 1 turn out to be negligible with values of 3.6×10^{-4} psi and 3.1×10^{-4} psi, respectively. The total pressure drop across all channels for both the nitrogen and feed air streams in heat exchanger 2 also results in negligible values of only 0.000179 psi and 0.000188 psi, respectively. It is also assumed that the tubing which carries the gases to and from the heat exchangers will also display negligible pressure drop. Therefore, there are no significant pressure drop considerations associated with this particular heat exchanger design.

5.5 Insulation

Insulation will be used in two places to insulate the BICUVOX membrane cell from the rest of the oxygen concentrator unit. A radiation reflective heat shield will be used inside the cell housing, between the housing wall and the resistance heating coils. The second location for insulation will be on the outside of the cell housing, and will prevent heat conduction from the cell housing to other components in the unit. Two types of insulation, for use on the exterior of the cell housing were considered. One type was a conventional, board insulation. The other type considered was the vacuum panel type.

5.5.1 Radiation Heat Shielding

The ceramic oxide membranes will be heated inside the stack by resistance heating wires or coils. To reduce the amount of heat transferred to the cell housing, a thin radiation barrier will be inserted between the heating coils. This will almost totally insulate the housing against radiative heat transfer from the coils. Most brands of heat shielding will reflect more than 97% of heat radiation. Some reflect as high as 99.9% of radiated heat. Using these heat shields, the radiation heat transfer to the cell housing can be neglected and the convective heat transfer from gases to the cell housing is the only consideration for heat transfer.

5.5.2 Cell External Insulation

Heat energy from hot gases inside the cell membrane is readily conducted through the magnesium-oxide (k value 30 W/m·K at 500°C) cell housing to the surrounding components. To protect heat sensitive components inside the oxygen-concentrator, the cell housing must be insulated. Many similar conventional insulation types exist with similar conductive qualities. One of these is BTU-block which is a molded, micro-porous panel, produced by Thermal Ceramics³⁹. It has a maximum continuous use limit of 1800°F (982°C), and a measured thermal conductivity at 1000°F (538°C) of 0.03 W/m·K. There are several drawbacks to using this type of insulation in the oxygen concentrator design. The first is the thickness of the material necessary to properly insulate the membrane stack. To achieve a cold face temperature at the outside of the cell stack housing of 80°F with a hot face temperature inside the cell housing of 1000°F, the insulation thickness required is 4.0 inches. Due to the size specifications of the final unit, this insulation is not efficient enough, on a per volume basis, for use in the design. Another drawback of the micro-porous panel insulation is the possible irritation to the eyes and skin and throat. Although there are no known long term health effects from this type of insulation, it must be a factor when selecting the proper insulation for the product design³⁸.

Vacuum technology offers an answer to the problems with micro-porous insulation thickness and health concerns. Porextherm's, Vacupor®³⁸ vacuum insulation panels provide excellent thermal insulating effects while posing no health issues. With a vacuum of 1 mbar, or 0.75 torr, it has a k value of 0.0048 W/m·K. Vacuum panels

require a core material to be inserted between the outer skins of the panel. This core material acts to support the walls of the panel against collapse due to external atmospheric pressure. The core material also inhibits the movement of gas molecules that remain in the panel after the vacuum is applied, reducing conductive heat transfer.

Vacupor®, with a core material of fumed silica, has an advantage over competing types of VIPs that use polystyrene and polyurethane foams for a core material. The advantage of the Vacupor® core material is that its conductivity does not appreciably increase with an increase in pressure, up to 100mbar.⁷³ While other products must be evacuated to 1 torr (1.3mbar) to reach the desired thermal conductivity value, Vacupor® requires only about 0.05 torr (0.067mbar). This results in significant cost reduction and life of the vacuum panel. Another advantage of Vacupor® that extends its service life above other products is that its core material will not outgas. Outgassing is the release of gasses that occurs with most materials subject to low pressure environments. The release of gasses inside the vacuum compartment greatly degrades the thermal insulating properties of the panel. Vacupor® can be used at constant temperatures of 500°C (932°F). With a panel thickness of 6.5cm (2.56in), and a hot face temperature of 773K, the cold face, or outer surface of the vacuum panel, will be less than 27°C (81°F). The following table shows thermal conductivity capacity.

Table 3: Thermal Conductivity Comparison

Insulation Type	R value (ft²·hr·°F/BTU·in)	Thermal Conductivity mW/(m·K)
Vacupor® VIP@ 1 mbar or 0.75 torr	30	4.8
Closed cell Polyurethane	4.1 - 7.6	19 - 35
Expandable Polystyrene (EPS)	4	36
Fiberglass batting	4	36

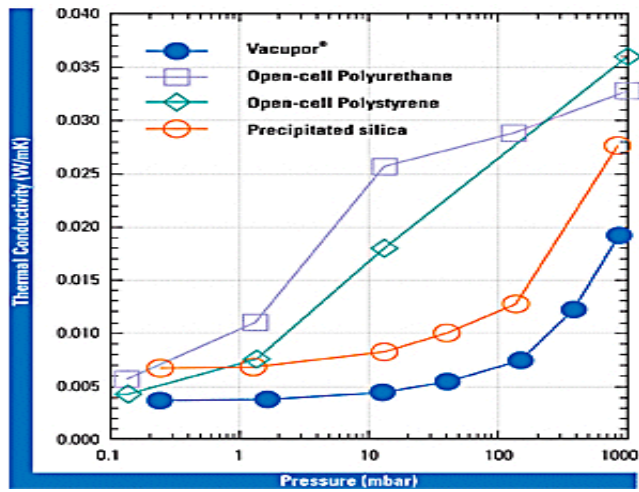


Figure 11: Effect of Pressure Rise on Thermal Conductivity³⁸

5.6 Feed Pump

Considerations for selection of a feed pump were size, cost, power usage, noise output, and safety for use in a breathing system. The pump chosen for the design would also be required to produce a minimum volumetric flow rate of 28 L/min. This feed flow rate is the minimum required to produce the specified oxygen product flow rate of 5 L/min, assuming 100% of the feed oxygen is transported across the membranes. The consideration of the highest priority was safety. The pump chosen for the project must be of a type that will not leak oil or other particles into the air stream. These particles would flow into the device and coat the ceramic membranes in the cell stack reducing, or destroying their ability to transport oxygen. Pumps considered safe for the oxygen concentrator device were either oil sealed, or of an oil-less design. Oil-less designs use ceramic bearings, and therefore, pose a low risk for release of foreign particles into the device. The next most important consideration was size. The final design size specification was that the entire oxygen concentrator fit inside a 7x7x12 in. space. This specification required that the smallest possible pump design be selected regardless of the potentially higher pump cost. When considering size, the pump power requirements must also be taken into account since they will affect the design battery size.

Taking into account the design parameters and afore mentioned considerations, the Thomas G12/07-N rotary pump, part number 50316, was chosen as the unit feed pump. It is oil-less, maintenance free, with no pulsation, and low vibration. The pump is

a permanent magnet type with a 12volt motor capacity. The flow rate is 18.5 L/min. at 1psi. The electrical rated load is 2.3W at an operating speed of 5400rpm, and a net weight of 1.1lb. The pump dimensions are 2x2.25x4.45 in. To meet the feed flow rate requirements of the design (28 L/min), two of these pumps are used with their airflows combined to give a total of 37 L/min.⁴⁸

5.7 Power Supply

The power for the operation of the device is supplied by a 12V lithium-ion battery. Direct current is used to allow the device to be portable. Lithium-ion chemistry is used for the battery because it has relatively large values of energy density (Wh/L) and specific energy (Wh/kg). These properties enable smaller batteries to be used for supplying the same amount of power that would require a larger size for competing battery chemistries. Another advantage is that lithium-ion batteries have a long, stable cycle life. They can be recharged completely in 3 hours and recharged to 95% capacity in 1.5 hours. The primary operating concern for this type of battery is the temperature. The melting point of the battery is 180°C so care must be taken to ensure that the membrane stack is sufficiently insulated to prevent the battery from becoming overheated.^{29, 30}

The battery was sized based on the total power required to operate the membrane stack, the feed pumps, and the heating element. The feed pumps each require current of 0.2 A with a voltage of 12 V. The power is the product of current and voltage. Together the feed pumps require 4.8 W. The heating element power is calculated by the product of the effective resistance and the square of the current. The heating element arrangement described above requires 66 W for the twenty minute startup period. The membrane stack requires a current to drive the oxygen flux across the membrane. The total power required by the membrane stack is the product of the total voltage drop and the current. The calculated value for the membrane power is 76.7 W.

The number of total Watt-hours required for the device is given by the total of the operating times for each component multiplied by the power required for that unit. The operating time for the pumps and the membrane stack is set as four hours and that for the

heating element is 20 minutes. The resulting total of required Watt-hours is 147.4 Wh. The specific energy of the lithium-ion battery is 150 Wh/kg, and the energy density is 400 Wh/L. Dividing the Watt-hour total by the specific energy and by the energy density gives the mass of the battery, 5.44 lb, and the volume of the battery, 0.92 L, respectively. New lithium ion battery technology could potentially triple specific energy and the energy density. The result of this technology would reduce the battery weight to 1.81 lb. and the battery volume to .31 L.

Additional power considerations for the study include the power required to operate process control equipment (i.e. temperature and flow rate sensors, switches, alarms) and the use of an AC/DC electrical converter in order to interchangeably use alternating and direct current power sources.

5.8 Controllers

Temperature, pressure, flow rate, voltage, alarms, and all other sensors are needed to maintain safe operating conditions in the device. They are also essential for user control such as input of flow rate. Audio and visual alarms should be present to ensure that the user is aware of any malfunction. The user would then be able to override the system by shutting it on or off. There should also be a visual display containing the set flow rate, the remaining battery life, and any malfunction warnings. The flow rate will be easily changed by adjusting a knob on the user interface panel.

The exact controller equipment specifications have not yet been explored. Future work will entail research on controller systems.

5.9 External Casing

The external casing material chosen for the oxygen concentrator was aluminum. Aluminum was chosen for its low cost, and low weight. It also offers high durability as opposed to plastics or fiberglass materials. Also, because of the breathing application of the oxygen concentrator device, the aluminum poses no breathing health or irritation effects that may exist with plastics or other materials. A wall thickness of 0.025 cm will provide the necessary strength without adding excessive weight to the unit.

5.10 Prototype Cost

Component costs are based on an actual manufacturer's cost of the part when quotes are available. When no actual price is available, the cost of the component is estimated from a similar device or material. If no similar devices are available for a cost comparison, a pure estimate is used. The Inconel electrode price is based on the bulk cost of Inconel which is sold at \$30.00 per pound. The battery cost is based on the cost of lithium ion batteries. The battery charger cost is an estimate from Home Depot for a Dewalt battery charger.

The resistance heating wire cost is based on the actual sales price from the manufacturer, More Electric Heating Association Incorporated. The cost of the vacuum insulation is an estimate based on the cost of conventional block insulation. Due to the extensive processing involved in producing the vacuum panels, as compared to block insulation, the cost of the vacuum insulation is estimated to be 1.5 times the cost for the same block insulation. The cost of the foil radiation shielding, Porextherm's High R Foil-Foil insulation, is the actual listed price of the product.

The cost of the heat exchanger is an approximation based on the cost of comparable conventional heat exchangers. The estimation for the heat exchanger is necessary because the exchanger design is based on new technology. No similar examples of the technology exist on the market to give a cost estimate. The external aluminum casing was estimated based on an average cost for aluminum cases of similar size. The cost given for the controls and alarms is a pure estimate. More research must be done in this area to give a better cost estimate of this item.

The pump prices are based on the actual pump prices from the Thompson Pumps distributor in Dallas, Texas. The pump cost per pump is \$234.00. The total cost for both pumps is then \$468.00. Also, pumps from this distributor have a 3-4 week shipping delay. A price estimate for the BICUVOX ceramic sheets is not available. No producer of BICUVOX sheets could be found to provide a closer approximation of the cost for this material. The sum of all costs and estimations gives an estimated unit cost of \$ 1785.50, with no consideration of manufacturing, profit margin or marketing costs. The following table gives the cost estimate of the ionic ceramic membrane device.

Table 4: BICUVOX Membrane Prototype Device Costs

Component	Cost (\$)	Basis
Inconel electrodes	30.00	assuming one lb per unit
Batteries	150.00	computer battery cost
Battery charger	50.00	
Resistance heating wires	1.00	\$0.80 / ft
Vacuum insulation	50.00	estimate
Foil radiation shielding	0.50	\$100 per 1000 ft ²
Heat exchanger	1000.00	estimate
External Casing	50.00	estimated from manufactured aluminum cases
Controls and alarms	100.00	
Pumps (2 ea)	468.00	estimated from prices of larger pumps
Ceramic BICUVOX	500.00	pure estimate, based on manufacturing process
Unit Cost	2500.00	

6.0 Pressure Swing Adsorption

6.1 Theory

In pressure swing adsorption (PSA), beds packed with an adsorbent (usually molecular sieve or zeolite) selectively adsorb a desired impurity under a pressure elevated above ambient conditions. PSA is used exclusively with gases, and most commonly for gas drying or air separation. In its basic form, a PSA system contains two equal-sized beds that undergo adsorption and desorption in alternating cycles. In addition, a smaller storage tank, maintained at a pressure slightly less than that of the compressed feed, is required to aid in continuous product production. A general flow diagram is shown below in Figure 12.

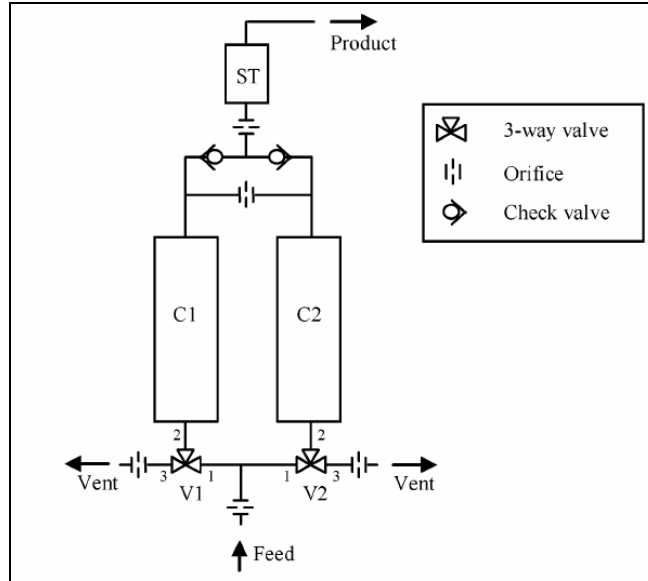


Figure 12: Flow Diagram for Air Separation PSA System⁵¹

Each column in the process is operating in one of two possible stages: 1) Pressurization/Production or 2) Vent/Purge. While one column is in Stage 1, the other column will always be in Stage 2. It is this alternation of cycles that allows a combination of two non-continuous processes to work together and produce a continuous product stream.

Initially the feed (air at ambient conditions) enters the system and is compressed up to the necessary operating pressure, which is generally three times ambient pressure⁵¹. In Stage 1, the compressed air flow is diverted to Column 1 through a three-way valve as seen in Figure 12. The check valve on the line connecting the column to the storage tank ensures that only product at a pressure greater than or equal to that of the storage tank will actually enter the tank. While Column 1 is being pressurized, its product stream of less than storage tank pressure will feed the top of Column 2 and act as a purge to aid desorption during the vent stage of Column 2.

When the product stream from Column 1 reaches storage tank pressure, the system will switch from feeding Column 2 to feeding the storage tank. Production of Column 1 into the storage tank will continue until the product stream falls below the

desired oxygen purity. Just before the product quality drops below the minimum acceptable value, feed to Column 1 will be stopped by a switch in Valve 1.

Stage 2 begins with the stoppage of feed into Column 1. The feed is diverted into Column 2, initiating Stage 1 for that column. In Column 1, the existing impure gas in the column is vented to the atmosphere. In addition, a purge from Column 2 will increase the desorption in Column 1. Column 1 will continue desorbing until the total pressure in the column equilibrates to atmospheric conditions. At this point, Stage 1 will stop in Column 2, and Stage 1 will begin again in Column 1.

If the production time of Column 1 can be designed to equal the desorption time in Column 2, the two stages can be alternated with a set timing to produce a continuous oxygen product of desired purity. The storage tank always remains at the elevated pressure, and a steady pressurized flow out of the tank is let down to atmospheric pressure and delivered to the user. A qualitative graph of the pressure histories of the two columns and the storage tank are shown below in Figure 13.

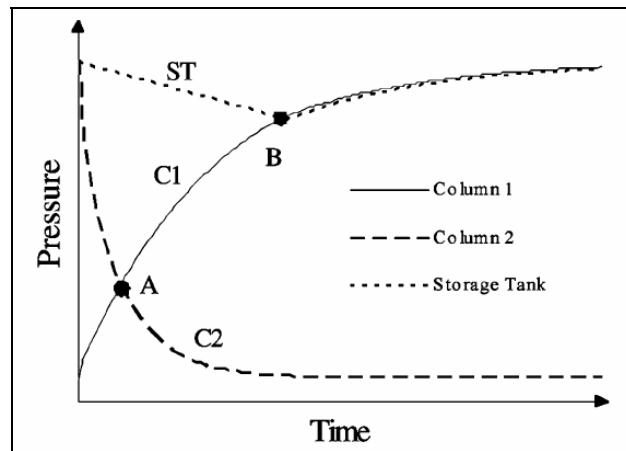


Figure 13: Pressure Histories of Columns and Storage Tank in PSA Device.

Point A represents beginning of purge into C1 into C2. Point B represents beginning of production of C1 into storage tank.⁵¹

A vacuum swing adsorption (VSA) process operates very similarly to PSA, except that in VSA, the columns operate at a pressure of just slightly above atmospheric, and the desorption step operates under a vacuum. In general, a VSA system will consume slightly less power than a PSA system⁵¹. However, the VSA system will require a greater volume for each column to match the product flow rate of PSA⁵¹. The goal of

this project was to increase the portability of an oxygen producing device, and the choice was made to pursue a PSA device since size will likely be a more limiting factor of portability than power requirement.

6.2 Model Performance

6.2.1 Nitrogen Removal

Adsorption of the components of air (78% N₂, 21% O₂, 1% Ar) onto an adsorbent is modeled by the Langmuir-Freundlich equation for multi-component adsorption. This equation⁵² is shown below in equation 11.

$$q_i = Q_{\max} \frac{\left(\frac{b_i}{\eta_i}\right)P_i}{1 + \sum_{j=1}^N \left(\frac{b_j}{\eta_j}\right)P_j} \quad (11)$$

where q_i is loading (mol/kg) of component i on the adsorbent, Q_{\max} is maximum loading (mol/kg) of any component onto the adsorbent, b_i is a constant for component i , N is the total number of components, η is a factor for interaction amongst components, and P_i is the partial pressure of component i .

For this model, the data in Table 5 was obtained by Santos, J.C. et. al.⁵¹ for Oxysiv 5 adsorbent manufactured by UOP.

Table 5: Adsorbent Data for Oxysiv 5⁹

Component	Qmax (mol/kg)	b (Pa ⁻¹)
N2	3.0704	1.02E-06
O2	3.0704	3.69E-07
Ar	3.0704	3.40E-07

In this model, η is assumed to equal unity, since interactions between oxygen, nitrogen, and argon are negligible. Therefore, equation 11 reduces to equation 12:


$$q_i = Q_{\max} \frac{b_i P_i}{1 + \sum_{j=1}^N b_j P_j} \quad (12)$$

The breakthrough time of the equilibrium front in the packed column is determined using equation 13⁵³

$$Q_F c_F t_x = q_F M L_x / L_B \quad (13)$$

where Q_F is the volumetric flow rate of feed, c_F is the concentration of solute in feed, t_x is the time the front has been traveling when at position L_x , q_F is the loading per mass of adsorbent in equilibrium with the feed concentration, M is the total mass of adsorbent in the bed, L_x is the distance traveled by front through bed, and L_b is the length of the bed.

The column is operated so as to allow the feed to reach equilibrium in the column, thereby making mass transfer effects negligible⁵³. In addition, the temperature and pressure in the column are assumed constant⁵¹. The goal of this setup is to produce a product stream of at least 90% pure oxygen. Since the column is operating ideally, the product stream will be free of nitrogen prior to the breakthrough of the front. The breakthrough will be achieved when $L_x = L_b$. Although the column can be designed for different breakthrough times, this column is designed for a breakthrough time of no less than 15 seconds. This allows for adequate time for gas to exit the columns and piping, and reduces wear and tear on the valves. UOP's Oxysiv 5 adsorbent (a 13-X type zeolite) is used in all modeling.

Utilizing equations 12 and 13, assuming ideal gas properties, assuming an inlet air composition of 78% N₂, 21% O₂, and 1% Ar, and desiring a breakthrough time of 15 seconds, it is calculated that the product stream from the column will consist of 95.26% oxygen and 4.74% argon. Two columns operating in the cycle of stages described previously allow continuous production of the fied oxygen product. Although this purity is clearly much higher than that of atmospheric air, the product of these columns alone does not meet the standards of patients receiving oxygen therapy who require at

least 99% pure oxygen. Therefore, additional steps must be taken to remove argon from the product stream.

6.2.2 Argon Removal

There exist two possible means of argon separation through use of a PSA device. One way operates similarly to the nitrogen removing columns described above in that the stream is allowed to come to equilibrium with the adsorbent. This method requires an adsorbent that has a significantly higher equilibrium loading preference for argon over oxygen. Unfortunately, argon and oxygen gas molecules possess very similar physical properties and yield nearly identical equilibrium isotherms. At least one study⁶⁵ has shown that separation of 95% oxygen and 5% argon to achieve 99% oxygen is possible using equilibrium based adsorption. However, the ratio of equilibrium loading for argon versus that of oxygen is only 1.2 at 30 degrees Celsius. The Langmuir isotherms for argon and oxygen can be seen below in Figure 14.

$$T = 30^{\circ} \text{ C.: } n_{Ar} = \frac{8.875C_{Ar}}{1 + 0.0041C_{Ar}} ; n_{O_2} = \frac{7.363C_{O_2}}{1 + 0.00307C_{O_2}}$$

$$T = 60^{\circ} \text{ C.: } n_{Ar} = \frac{5.222C_{Ar}}{1 + 0.0025C_{Ar}} ; n_{O_2} = \frac{4.155C_{O_2}}{1 + 0.00166C_{O_2}}$$

$$T = 90^{\circ} \text{ C.: } n_{Ar} = \frac{3.206C_{Ar}}{1 + 0.00117C_{Ar}} ; n_{O_2} = \frac{2.629C_{O_2}}{1 + 0.00108C_{O_2}}$$

Figure 14: Langmuir Equilibrium Adsorption Isotherms for Argon and Oxygen⁶⁵

Most PSA systems for separating gases have a ratio of the adsorbed component versus the non-adsorbed component of at least 4 or 5. Therefore, although this method can achieve the desired purity of 99% oxygen from a 95% oxygen feed stream, the recovery will be poor since nearly equal amounts of oxygen and argon are adsorbed. Until an adsorbent is found that can achieve a much higher ratio of equilibrium loading for argon and oxygen, this method will not be practical for efficient purification of a 95% oxygen stream.

The second, and more common, method for separating gases with similar isotherms involves exploiting the differences in the rates of adsorption for each molecule. Although the two components may achieve near equal loading on the adsorbent if allowed to reach equilibrium, one component usually adsorbs more quickly than the other. This phenomenon occurs due to differences in the effective (combined macropore and micropore) diffusivities of the components in the adsorbent being used. Therefore, a column can be created and timed to operate so that the column stops producing when a relatively large amount of one component has adsorbed while the other component still remains largely in the interstitial unadsorbed gas. The shorter cycle times associated with the kinetic based PSA devices allows the manufacturer to use a smaller column, which reduces overall product cost.

Rege and Yang⁶⁶ have demonstrated that this kinetic separation is possible in a 95% oxygen stream to yield a 99% pure oxygen stream when adsorption occurs on Bergbau-Forschung Molecular Sieve Carbon (BF-MS). The model used to determine the rate of adsorption in the Rege and Yang study is not specifically listed, but is assumed to follow the Linear Driving Force (LDF) model¹⁸. The governing equation for this model is shown below in Equation 14

$$\frac{\partial \bar{q}}{\partial t} = \frac{15D_e}{R_p^2} (q_{Rp} - \bar{q}) \quad (14)$$

where \bar{q} is the average loading of component on the adsorbent, t is time, D_e is the effective intraparticle diffusivity, R_p is the radius of a particle, and q_{Rp} is loading at particle surface.

The values of D_e/R_p^2 for oxygen and argon are calculated by Rege and Yang to be $5.2 \times 10^{-3} \text{ s}^{-1}$ and $1.7 \times 10^{-4} \text{ s}^{-1}$, respectively. Clearly, oxygen has a higher effective diffusivity than argon when being adsorbed onto the MSC. A plot of fractional uptake versus time on this sieve is shown below in Figure 15.

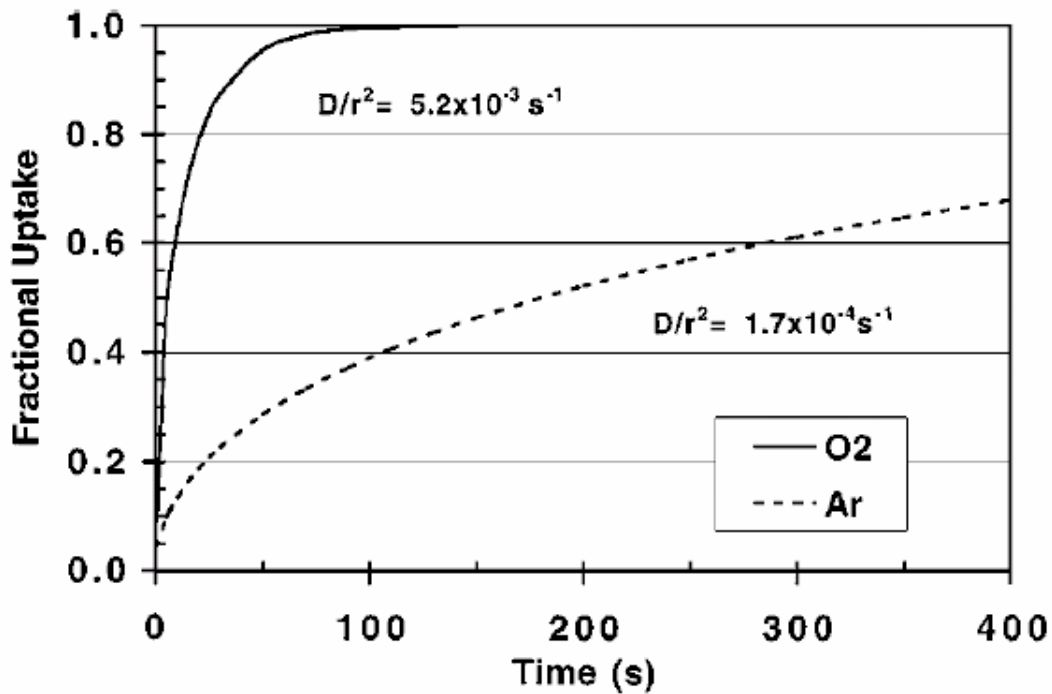


Figure 15: Fractional Uptake Versus Time for Oxygen and Argon on Bergbau-Forschung Carbon Molecular Sieve⁶⁶

Since oxygen is both the desired product and the component being adsorbed, the production cycle of the PSA system is slightly altered from that of the nitrogen adsorbing device described earlier. Rege and Yang⁶⁶ describe the cycle steps as follows: Step (I) pressurization with the feed gas (mixture of 95% O₂ and 5% Ar on molar basis); (II) high pressure adsorption with feed gas, i.e., feed step; (III) high pressure cocurrent purge with part of the O₂-rich product obtained in step (IV); (IV) countercurrent blowdown to a low pressure.

Figure 16 below depicts the steps in the adsorption cycle, as described above.

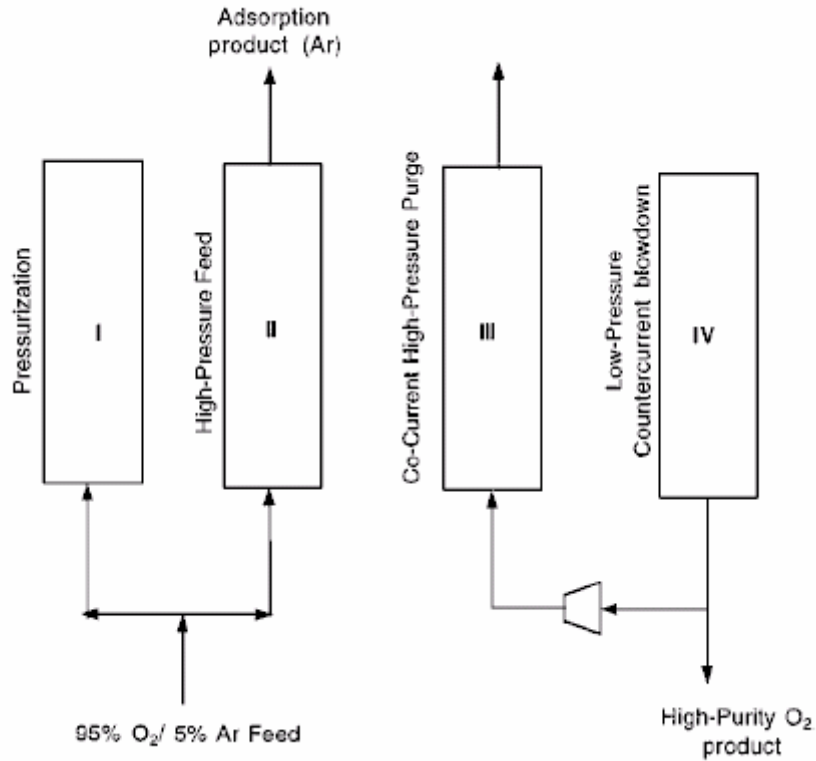


Figure 16: Steps of Oxygen Adsorbing PSA Cycle.⁶⁶

High pressure = 2 atm, low pressure = 0.2 atm.

6.3 Column Sizing

For the purposes of this study, the findings of Rege and Yang concerning the performance of a kinetic-based oxygen and argon separator are assumed accurate. In the results of Rege and Yang, it is seen that a device with a high pressure of 2 atm and a low pressure of 0.2 atm yields a product of 99.07% oxygen purity. This operational scenario offers 52.22% oxygen recovery and produces 0.01157 kg of product (oxygen) per kg of adsorbent in the bed. Therefore, the desired product flow rate of 5 lpm at STP (0.393 kg/min) requires 33.9 kg (74.6 lbs.) of adsorbent per column. The average carbon molecular sieve bulk density is 0.68 kg/L⁶⁷. This density yields a column volume of 49.9 liters per column, or about 100 L for the combined volume of the two columns required to run a continuously producing PSA system. Since the total oxygen recovery on this

system is only 52.22%, an initial feed rate of 9.9 lpm is required to produce a full 5 lpm product.

To provide 9.9 lpm to the oxygen and argon separating columns, the oxygen and nitrogen separating columns must produce a 9.9 lpm product stream. Assuming an equilibrium driven separation, using Equations 3.2 and 3.3 for modeling, and desiring a breakthrough time of 15 seconds, a mass of 0.95 kg of UOP Oxysiv 5 adsorbent is required per oxygen and nitrogen separating column. Assuming that 10% of the product stream is used to purge the column, a feed air flow rate of 79.2 lpm is required to produce a product of 9.9 lpm of 95% oxygen purity from the oxygen and nitrogen separating columns.

6.4 Practicality of Device

It is obvious from even a preliminary examination that the size of the combined oxygen nitrogen and oxygen argon separating columns into one device yields a machine that is too large and too heavy to be portable. There is little demand for an in-home oxygen producing device that is not portable, since many medical oxygen users use the oxygen only when they move around. Therefore, the method of generating 99% pure oxygen through two PSA cycles in series must be modified to provide a useful service to oxygen users.

Many medical oxygen users achieve portability of their oxygen supply through use of small cylindrical aluminum tanks filled with highly compressed oxygen.⁴³ These cylinders require no power supply and can be adjusted to produce as high a flow rate as needed by the user. The cylinders are delivered by a provider to the user's home on a regular basis, at which time the user exchanges used (depressurized) cylinders for new ones. This method of delivery contains the inherent limitations that the user must work around the schedule of the delivery company, and that the user is limited to the number of cylinders delivered each time. These limitations can be resolved by use of an in-home device that can refill/re-pressurize the portable cylinders with 99% pure medical oxygen. At this time, no such product exists. Hence, a sizeable unsatisfied demand currently

exists for a modified version of the previously described PSA based device to be used as an in-home bottling machine.

6.5 Bottling Device

A standard portable E-size cylinder, shown in Figure 17 and used by most patients on oxygen therapy, has a volume of 6.9 liters and is pressurized with 99% pure oxygen up to 2200 psi. At this pressure and volume, one cylinder can provide oxygen at a rate of 5 lpm for 205 minutes. However, most patients only use 5 lpm when they are actively moving around. Therefore, a cylinder lasts longer for a patient who is not continuously mobile for 205 minutes. The design for our bottling device presumes that the user desires to fill two full E-size cylinders at a time. This allows the user at least 410 minutes, or almost 7 hours, of continuous mobility. The bottling device produces the 99% oxygen continuously at 5 lpm. Therefore, as long as the user does not breathe more than 5 lpm continuously, the bottling device keeps up with the demand of the user.



Figure 17: E Size Oxygen Cylinder⁶⁸ Which Provides 205 Minutes of Oxygen at 5 L/min.

To minimize filling time of the E-size cylinders, the bottling device produces into one large storage tank at a pressure higher than 2200 psi. By maintaining the large storage tank pressure well above 2200 psi, the small E-size cylinder can be connected to the large tank and, because of the difference in pressure, oxygen rapidly flows from the large tank into the small cylinder. The large tank is large enough and at a high enough pressure that two of the E-size cylinders can be filled up to 2200 psi from the large tank, and the final pressure of the large tank will still be higher than 2200 psi.

An H-size oxygen tank has a volume of 58 liters and is used as the large storage tank described previously. It is desired to ensure that the pressure in the large tank never drops below 2500 psi. This maintains a pressure difference of at least 300 psi between the large tank and the E-size portable cylinders, and allows the large tank to provide a minimal amount of emergency oxygen in case the user needs oxygen but has forgotten to completely refill the large tank. To provide enough oxygen to fill two E-size cylinders and still remain above 2500 psi, the large H-size tank is initially filled up to 3021 psi.

Assuming the H-size tank and the E-size cylinders are connected by a six inch long $\frac{1}{4}$ inch diameter smooth pipe, and that the flow controlling valve opens instantly, it takes 5.1 seconds to fill the first E-size cylinder to 2200 psi. This leaves the H-size tank at a pressure of 2761 psi. When the second E-size cylinder is connected in the same manner, it takes 5.2 seconds to fill it to a pressure of 2200 psi. This leaves the H-size tank at the desired final pressure of 2500 psi.

As described previously, the bottling device fills the large tank at a rate of 5 liters per minute of oxygen. To fill the large H-size tank, this feed is pressurized from its outlet at 14.7 psi to the maximum H-size tank pressure of 3021 psi. Assuming the H-size tank is initially at 2500 psi and a fill rate of 5 standard liters per minute, it requires 410 minutes to fill the large tank to its maximum pressure.

6.6 Compressors

Initially, the feed to the nitrogen removing columns requires pressurization from atmospheric pressure up to 45 psia. This pressure difference at 79.2 lpm is created using a $\frac{1}{2}$ horsepower Thomas Pump⁴⁸ # GH-505B. After exiting the nitrogen adsorption

columns, the 9.9 lpm stream is let down to 2 atm before entering the argon removing columns. The evacuation of the columns in the oxygen argon separation cycle occurs at a sub-atmospheric pressure of 0.2 atm and a flow rate of 7.987 lpm. This depressurization is handled by a 0.02 hp Thomas vacuum pump⁴⁸ # 7011-0008. A fraction of this depressurized stream is re-pressurized to 2 atm for use as a purge. The purge stream flow of 2.987 L/min is pressurized by a 1/7 horsepower Thomas pump⁴⁸ # 607CD32. The final product of 99% oxygen at 5 L/min is pressurized to 3021 psi to fill the H-size storage tank. This compression is achieved by a Max Air 35⁶⁹ 3 horsepower compressor. The total power consumption of all compressors is 3.66 horsepower, or 2.74 kW. Assuming that the bottling machine only needs to be running for 12 hours per day, this machine consumes power at a rate of 32.8 kWh per day, or 1018 kWh per month.

6.7 Air Drying

Moisture in the air feed to the bottling device acts as a poison for the Oxysiv 5 adsorbent. The water molecules compete for adsorption sites with nitrogen, but cannot be removed through the same depressurization cycle as nitrogen. Therefore, the water moisture in the incoming air needs to be removed as extensively as possible to increase the longevity of the adsorbent.

Silica gel provides a low cost method for removing water moisture from air. Since silica gel is easily regenerated by heating, only enough silica gel to dry one bottling cycle is required. The water equilibrium capacity (40%) was used to find how much desiccant would be needed to dry air with a humidity level of 100% for 5 hours. Humidity levels of 100% were used so that the column could safely operate for 5 hours at all but harshest conditions. The following equations were used to size desiccant dryer. Equations 15 and 16 below are used to determine the necessary volume of desiccant. In equation 15, H is the grams of water and carbon dioxide per liter of air at 100% humidity. The mass of carbon dioxide was assumed constant at 0.03% of air.

$$Mass = H * airFlowrate \tag{15}$$

$$Volume = \frac{Mass}{\rho} \tag{16}$$

The necessary amount of silica gel to dry the 79.2 L/min feed rate is 4.9 lbs. of silica gel to dry the feed for one bottling cycle. An electrical heating element is coiled within the silica gel canister to provide the heat necessary to recharge the gel upon termination of the feed. This heating element is automatically turned on at the end of each bottling cycle. The heating element heats the gel for a certain amount of time, and the bottling device cannot begin producing until the necessary time for regeneration has passed.

The precise location of the heating element within the bed, the heating time required, and the method of allowing the desorbed water vapor to exit the canister have not been thoroughly analyzed in this work. A more detailed study of the drying mechanism is required to ensure the bottling device operates at the highest possible efficiency.

6.8 Materials

The body and fittings of each column, drying canister, and storage tank in the device are made of aluminum. The piping is 1/2" Schedule 40 copper piping. Each set of columns requires two check valves between the columns and the storage tank, and two 1/2" three-way solenoid valves to control the feed and venting of each column. The valves are electronically time-controlled by a small computer. Small fans are used to circulate air over the fins on the compressor to ensure near-isothermal compression. The device is built on a steel frame and is enclosed with a plastic cover.

A breakdown of the costs of each of the objects within the device is shown below in Table 6.

Table 6: Itemized Cost of Components of Bottling Device

Parts Breakdown	Price	N₂ removal section	Ar removal section	Combined Costs
Metal	\$/ft ²	ft ²	ft ²	Total Cost
Adsorption Columns (Aluminum) ⁵⁵	1.5	2.13	14.88	\$ 25.51
Low Pressure Storage Tank (Aluminum) ⁵⁵	1.5	1.13		\$ 1.70
Dryer canister (Aluminum) ⁵⁵	1.5	2.30		\$ 3.45
Frame (Steel) ⁵⁶	2	15	15	\$ 60.00
Piping	\$/ft	ft	ft	Total Cost
1/2" Sch. 40 Copper ⁵⁷	3.6125	6	10	\$ 57.80
Packing	\$/lb	lb	lb	Total Cost
Oxysiv 5 adsorbent ⁵⁸	5.5	4.21		\$ 23.16
BF-CMS ⁶⁷	3		148.00	\$ 444.00
Silica gel ⁵⁹	2	4.9		\$ 9.80
Items	\$/item	Number of items	Number of items	Total Cost
Feed Compressor ⁴⁸	230	1		\$ 230.00
Vacuum Pump ⁴⁸	100		1	\$ 100.00
Purge Compressor ⁴⁸	150		1	\$ 150.00
Tank fill Compressor ⁶⁹	2500		1	\$ 2,500.00
High Pressure Storage Tank ⁷⁰	150		1	\$ 150.00
Fan	5	2	2	\$ 20.00
3-way solenoid valve ⁴⁷	86	2	2	\$ 344.00
Check valve	20	2	2	\$ 80.00
Computer	20	1		\$ 20.00
Casing	100	1		\$ 100.00
Total Final Cost				\$ 4,319.42

A breakdown of the weights of each of the components of the machine is shown below in Table 7.

Table 7: Weights of Individual Components of Bottling Device

Parts Breakdown	Weight	N₂ removal section	Ar removal section	Combined Weights
Metal	lb/ft ²	ft ²	ft ²	Total Weight (lbs)
Adsorption Columns (Sch. 40 Aluminum)	1.5	2.13	14.88	25.51
Low Pressure Storage Tank (Sch. 40 Aluminum)	1.5	1.13		1.70
Dryer canister (Sch 40 Aluminum)	1.5	2.30		3.45
Frame (Steel)	3	10.00		30.00
Piping	lb/ft	ft	ft	Total Weight (lbs)
1/2" Sch. 40 Copper	0.75	10	6	12.00
Packing	lb/column	columns	columns	Total Weight (lbs)
Oxysiv 5 adsorbent	2.1	2		4.20
BF-CMS	74		2	148.00
Silica Gel	4.9	1		4.90
Items	lb/item	Number of items	Number of items	Total Weight (lbs)
Feed Compressor	45	1		45.00
Vacuum Pump	2		1	2.00
Purge Compressor	11		1	11.00
Tank fill Compressor	85		1	85.00
High Pressure Storage Tank	135		1	135.00
Fan	0.5	2	2	2.00
3-way solenoid valve	1.5	2	2	6.00
Check valve	1.5	2	2	6.00
Computer	1	1		1.00
Casing	8	1		8.00
Total Final Weight (lb)				530.76

Figure 18 shows the process flow diagram for the entire pressure swing adsorption device.

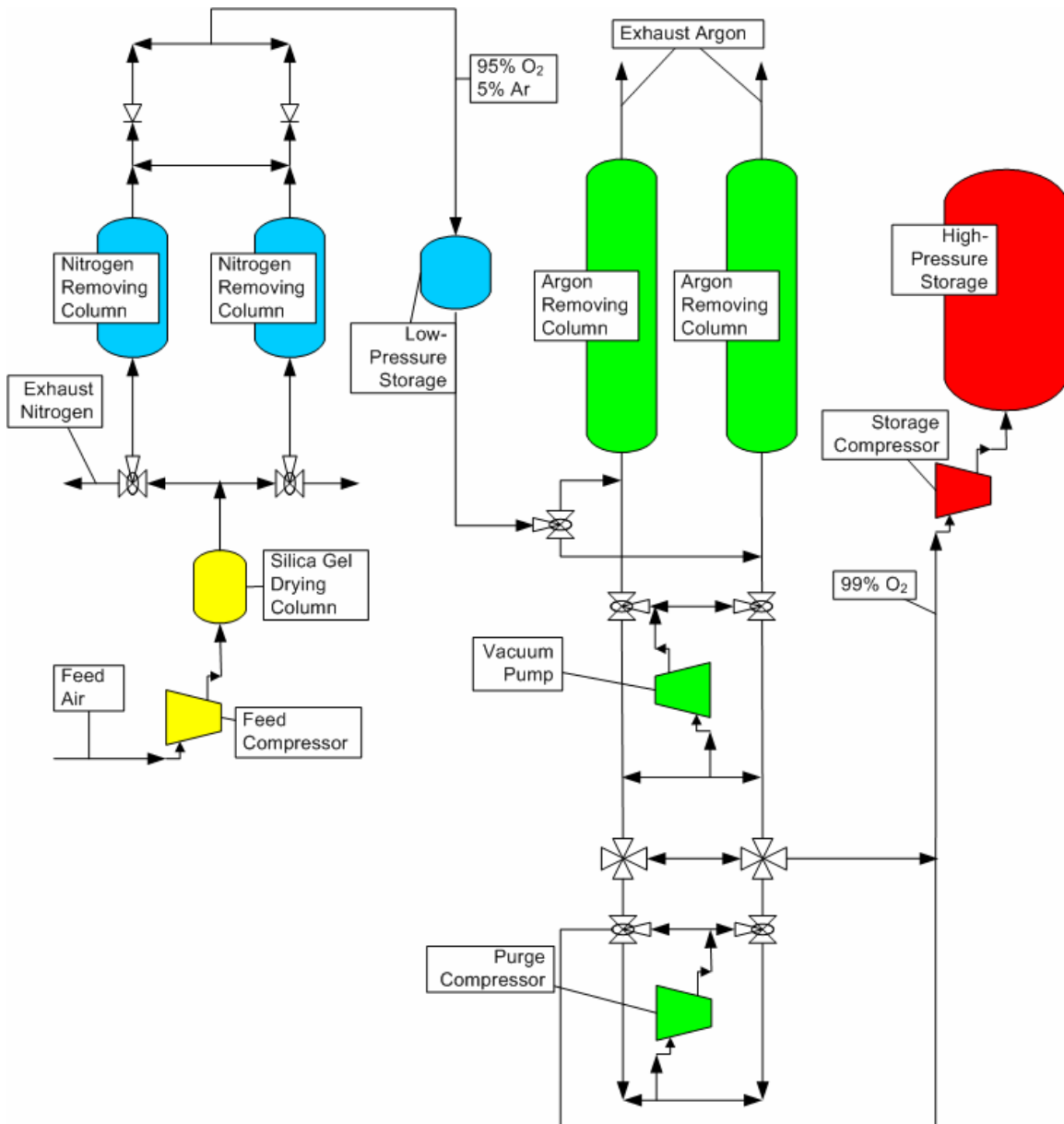


Figure 18: Pressure Swing Adsorption Process Flow Diagram

7.0 Marketing and Cost Analysis

7.1 Price Determination

In order to estimate the price for the oxygen concentrators developed in this project based on the demand, the price and demand the economic model shown below was used:

$$\alpha P_1 d_1 = \beta P_2 d_2 \quad (17)$$

where α is a function of the advertising level and time, P and d are the selling price and demand, β is a function of consumer happiness and time, and the subscripts 1 and 2 refer to the designed device and the competitor's device, respectively.

7.1.1 The Alpha Function

The alpha function, $\alpha(y,t)$, describes how much time it will take for the public to become aware of the products designed. In order to increase demand, advertising can be used to increase the public's awareness of our product. The following equation was used to describe this relationship:

$$\alpha(y,t) = 1 - \left(\frac{y \times t}{y \times t + 1} \right) \quad (18)$$

where y is the level of advertising and t is the time in years that the product has been out on the market. As the level of product advertising is increased, the value of the alpha function increases. Advertising's effect on the alpha function is shown in the graph below.

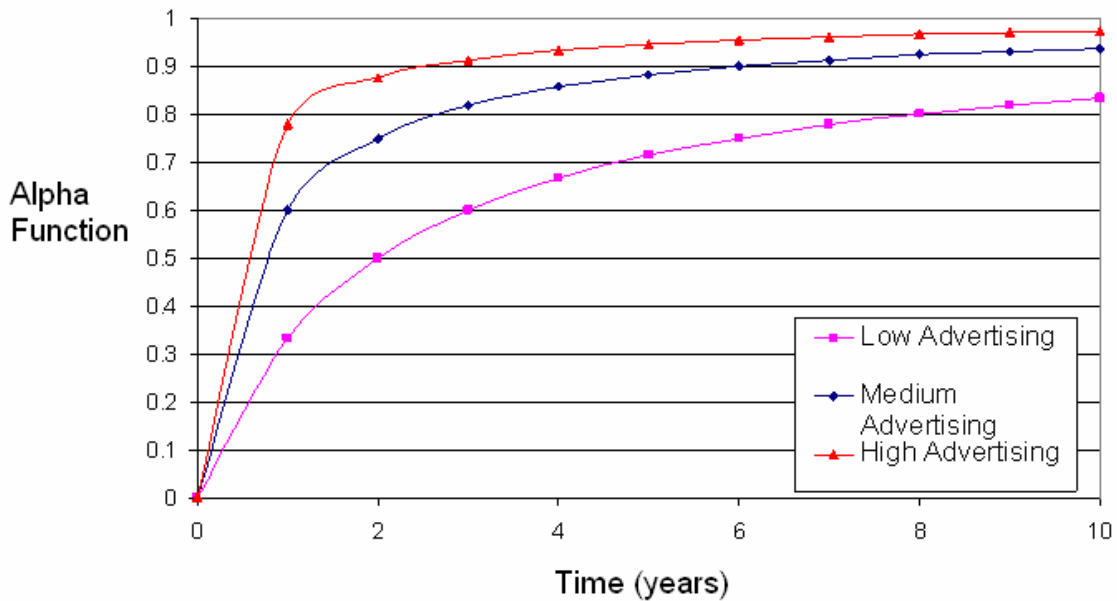


Figure 19: Effect of Advertising on the Alpha Function

The limit of the alpha function for all advertising values is always 1. Increasing the advertising level simply decreases the time for it takes for the majority of the market to become aware of our product. The advertising level for the model was set so that 90% of the public was aware of the designed products after three years.

7.1.2 The Beta Function

The beta function, $\beta(k,t)$, is used to predict the likelihood that a consumer would choose to purchase the designed product. The beta function is a function of the happiness ratio between the designed product and the competitors' products and time in years. The equation used to find the value of the beta function is given below:

$$\beta(k,t) = 1 - k_1 \left(\frac{Ht}{Ht + 1} \right) \quad (19)$$

where H is the happiness ratio between the two products, t is time in years, and k is a constant. Happiness is defined as how much joy or utility the consumer will gain by buying the products designed in this project. As the happiness of our product increases, the final value of the beta function decreases. This decrease in the beta function will cause an increase in the demand for the designed product. This effect is shown in the figure below.

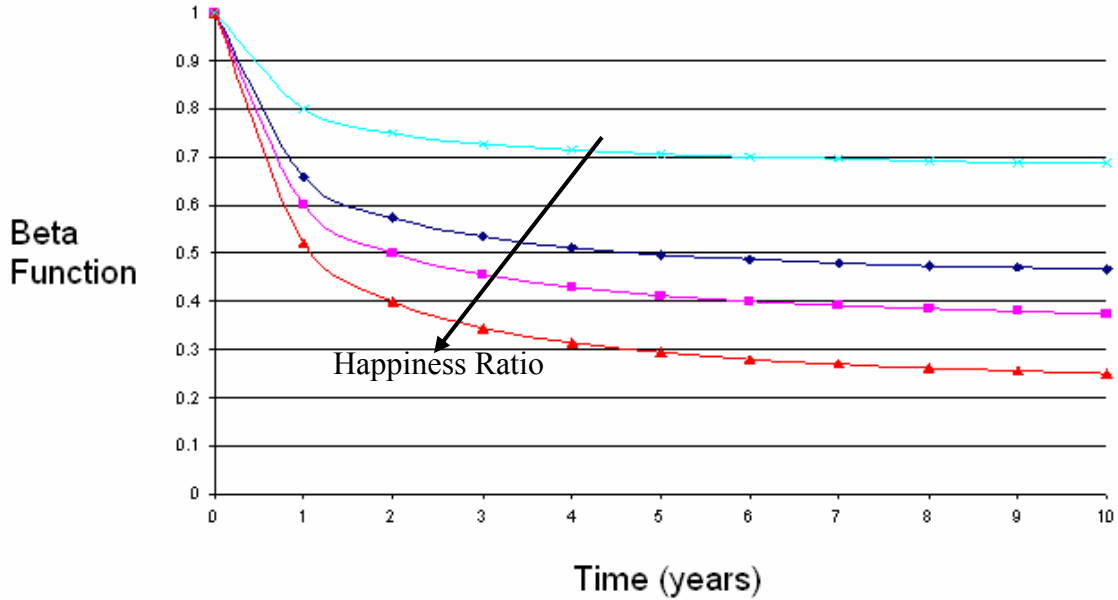


Figure 20: Beta Function vs. Time for Various Happiness Ratios

7.1.3 Happiness Determination

The happiness of each product was determined by comparing the properties of our product to the minimum or maximum acceptable values. Happiness factors, such as portability and durability were determined and weighted in order of importance. The deviation from the minimum acceptable value was calculated for each factor by comparing the value of each property to the maximum attainable value and the minimum acceptable value. The deviation from the minimum acceptable value for was found for each factor with the following equation:

$$Dev = \frac{Pr oduct Value - Min Value}{Max Possible Value - Min Value} \quad (20)$$

Each deviation was weighted on a scale of consumer importance. The happiness value for each product was found by summing the deviation of each factor. This was also done for the leading competitor for each of the three products. The happiness ratio was found by comparing the happiness value of each product to its main competitor. The happiness values for the three products designed are shown in the following tables.

Table 8: Happiness Values for 95 % Oxygen Concentrator

Happiness Factors	Importance	Normalized Weight	Product Deviation	Weighted Deviation	Competitor Deviation	Weighted Deviation
Reliability	10	0.167	1.000	0.167	0.818	0.136
Size	7	0.117	0.700	0.082	0.700	0.082
Weight	8	0.133	0.320	0.043	0.320	0.043
Portability	6	0.100	0.450	0.045	0.300	0.030
Durability	4	0.067	0.400	0.027	0.400	0.027
Noise	5	0.083	0.200	0.017	0.200	0.017
Purity of Air	9	0.150	0.000	0.000	0.000	0.000
Appearance	2	0.033	0.400	0.013	0.300	0.010
Battery life	5	0.083	1.000	0.083	0.000	0.000
Variable Flow-rates	4	0.067	1.000	0.067	1.000	0.067
					Product Happiness	0.543
					Competitor Happiness	0.411

Table 9: Consumer Happiness for 99% Oxygen Bottle Refiller vs. Delivered Oxygen

Happiness Factors	Importance	Normalized Weight	Product Deviation	Weighted Deviation	Competitor Deviation	Weighted Deviation
Reliability	10	0.167	1.000	0.167	1.000	0.167
Size (bottle)	7	0.117	1.000	0.117	1.000	0.117
Weight (Bottle)	8	0.133	1.000	0.133	1.000	0.133
Portability(bottle)	8	0.133	0.400	0.053	0.600	0.080
Durability	7	0.117	0.400	0.047	0.000	0.000
Noise	5	0.083	0.500	0.042	0.330	0.028
Purity of Air	9	0.150	1.000	0.150	0.000	0.000
Appearance	2	0.033	0.300	0.010	0.250	0.008
Variable Flow-rates (bottle)	4	0.067	1.000	0.067	0.500	0.033
Privacy	5	0.083	1.000	0.083	0.000	0.000
Ease of use	6	0.1	0.5	0.050	1.000	0.100
Ability to Use bottles at home	6	0.1	1.000	0.100	0.400	0.04
					Product Happiness	1.018
					Competitor Happiness	0.706

Table 10: Consumer Happiness for Membrane Concentrator vs. AirSep Lifestyle

Happiness Factors	Importance	Normalized Weight	Product Deviation	Weighted Deviation	Competitor Deviation	Weighted Deviation
Reliability	10	0.147	0.600	0.088	0.000	0.000
Size	7	0.103	0.006	0.001	0.976	0.100
Weight	8	0.118	0.100	0.012	0.500	0.059
Portability	8	0.118	0.400	0.047	0.600	0.071
Durability	7	0.103	0.400	0.041	0.000	0.000
Noise	5	0.074	0.500	0.037	0.330	0.024
Purity of Air	9	0.132	1.000	0.132	0.000	0.000
Appearance	2	0.029	0.300	0.009	0.250	0.007
Battery life	8	0.118	0.667	0.078	0.166	0.020
Variable Flow-rates	4	0.059	1.000	0.059	0.500	0.029
					Product Happiness	0.504
					Competitor Happiness	0.310

7.1.4 Demand as a Function of Selling Price

For our device the maximum demand was assumed to be 12,000 devices per year. This number was found from the overall sales that Airsep has had since their product arrived on the market. In order to find demand for our product as a function of price the following equations were combined

$$\gamma = \frac{\beta}{\alpha} \quad (21)$$

and

$$d_2 = D - d_1 \quad (22)$$

where D is the total demand .

Then solving for d_1

$$d_1 = \frac{\gamma P_2 D}{P_1 + \gamma P_2} \quad (23)$$

Assuming that P_2 and D are constant, d_1 is now a function of our selling price.

TCI was found as a function of selling price by setting the capacity of each plant to the maximum demand value at that price. The direct and indirect costs of the TCI were found as a percentage of the purchased equipment costs, as found in Peters and Timmerhaus⁷¹. The net present worth during the 10th year of the project was then found from the TCI and the cash flow, which was determined by multiplying the demand for

our product by the selling price of our product. The TCI for the membrane oxygen concentrator device is given below as an example. The TCI for the other two devices was found using the same method and can be found in Appendix F.

Table 11: TCI Calculation for Membrane Device

Capital Investment for Portable Oxygen Device		
	Percent of Equipment Cost	
Direct Costs		
Purchased equipment delivered	100	\$30,000,000
Purchased-equipment installation	45	\$13,500,000
Instrumentation and controls	18	\$5,400,000
Piping	16	\$4,800,000
Electrical systems	10	\$3,000,000
Buildings	25	\$7,500,000
Yard Improvements	15	\$4,500,000
Service facilities	40	\$12,000,000
Total direct plant cost	269	\$80,700,000
Indirect costs		
Engineering and supervision	33	\$9,900,000
Construction expenses	39	\$11,700,000
Legal expenses	4	\$1,200,000
Contractor's fee	17	\$5,100,000
Contingency	35	\$10,500,000
Total indirect plant cost	128	\$38,400,000
Fixed Capital Investment	397	\$119,100,000
Working Capital (15% of TCI)	70	\$21,017,647
Total Capital Investment	467	\$140,117,647

The selling price was then found by finding the selling price that returned the highest NPW.

7.2 Correcting the Model Error and Results

When solving for the selling price by maximizing the FCI an error in the model was discovered. As the difference in the selling prices of the two products grew, so too did the error in the model until the results were unreasonable. In order to remove this error the Beta function was adjusted to increase when the selling price of our product approached and passed twice the selling price of our competitors. This was done with the following equation.

$$\text{If } \frac{P_1}{P_2} > 1.5 \tag{24}$$

then
$$B = B_o + \frac{p_1}{(k \times p_2)} \tag{25}$$

Where B_o is the value of B previously calculated using equation 19. This correction in the equation makes it possible to obtain an optimum Selling price. The optimum selling prices and resulting NPW and TCI are shown below.

Table 12: Optimum Selling Price, TCI, and NPW of the Three Devices

Device	90% Oxygen Concentrator	99% Oxygen Concentrator	Membrane Concentrator
Selling Price	\$1800	\$18,500(Base) \$27,000 (with Electricity)	\$11,000
TCI	\$4.7 million	\$80 million	\$133 million
NPW (10 years)	\$3.4 million	\$105 million	\$166 million

The membrane concentrator returns the highest NPW although it also has the highest TCI. One of the reasons the membrane concentrator has a very high TCI is the high amount of research needed to develop processes to mass-produce micro-channel heat exchangers as well as the ceramic membranes. In future works examining the economic potential of the three product designs several new aspects, shown below, should be examined.

- Offer to rent the tank filling device at a monthly rate
- Extensive market research should be conducted to improve happiness factors and weight ratios
- Price of advertising vs. benefit of advertising
- More accurate FCI calculations
- Estimating the cost of researching processes to mass produce micro-channel heat exchangers and ceramic membranes.

8.0 Device Approval Regulations

8.1 FDA Regulations

In order to get a medical device approved for sale in the United States, federal regulations must be followed as outlined by the Food and Drug Administration. These regulations ensure the general public that only safe medical devices ever make it to the market. The following sections will outline the procedure required to gain FDA approval of a portable oxygen generation device.

The FDA classifies portable oxygen generators as a Subchapter H Medical Device, Part 868 Anesthesiology Device, Subpart F Therapeutic Device, and finally as a Sec. 868.5440 *Portable Oxygen Generator*. The FDA defines a portable oxygen generator as being a device that releases oxygen for respiratory therapy by physical means or by a chemical reaction¹⁰.

There are three classes of devices within the FDA. Class I devices are those that pose the least risk to the patient, such as a tongue depressor, while Class III devices are those that are vital to human health and pose the greatest risk to the patient. Portable oxygen generators are classified as Class II devices. Therefore, the device is subject to a Pre-market Notification, otherwise known as a 510(k) application.

A Pre-market Notification requires that the device displays “substantial equivalence” to a predicate device that already exists on the market. After choosing a predicate device for comparison, the new device must prove to be at least as safe, effective, and intended for the same use as the predicate device. Substantial equivalence of a new technology can be achieved if the new technology is intended for the same use as the predicate device; and, if there are factors that could affect the safety and effectiveness of the new device, there must be accepted scientific procedures to determine if these factors have been diminished, and there must also be supporting data proving that these factors have not been diminished by the new technology¹¹.

After finding a predicate device and obtaining the necessary data to prove substantial equivalence, the Pre-market Notification (510k) application can be submitted. The application packet should include all of the following items to be considered for approval by the FDA¹²:

- Device name and class (I, II, or III)
- Establishment registration number
- Intended use and directions for the device
- Photographs or engineering drawings
- Proposed labels and advertisements
- Identification of predicate device used for substantial equivalence
- Statement declaring equivalence to the existing device with supportive data
- Descriptive data are also needed to understand the new device's intended use, physical composition, method of operation, specifications, and performance claims
- Performance testing data to determine substantial equivalence of the predicate device (may also need testing data of the predicate device itself)
- Data showing the manufacturer has considered the consequences the new technology could have on safety or effectiveness
- Statement declaring truthfulness and accuracy of all submitted data
- Any additional information requested by the FDA to approve substantial equivalence
- A 510(k) summary
- Financial certification
- Standard fee of \$3,502 submitted at or before the time of the 510(k) submission
- Fee is not to be enclosed with the 510(k) application

For all Class II devices, the 510(k) application must be submitted at least 90 days before planning to market in the United States. For the fiscal year 2003, the average total review time, including any wait period, was 96 days. For that particular year, 4,247 original 510(k) applications were received¹³.

After substantial equivalence has been proven to the FDA by submitting the Pre-market Notification packet, the portable oxygen concentrator device can be legally marketed in the United States. Even after the device goes to market, specific post-market surveillance controls must be upheld by the company. A quality system of controls is in

place to ensure that the company keeps producing a quality medical device even after approval. The company must also abide by the Medical Device Reporting system, which requires the company to report any safety mishaps, failures, or injuries which have occurred while the device is in operation. All of these FDA regulations help protect consumers from fraudulent claims and scams concerning medical devices.

8.2 FAA Regulations

The Federal Aviation Administration (FAA) has imposed numerous regulations concerning the use of personal oxygen therapy equipment on board aircraft. Federal regulation prohibits the use of portable compressed or liquid oxygen tanks on all flights in the United States. However, some airlines do provide oxygen tanks to passengers who require supplemental oxygen. The tanks cost the passenger approximately \$75 per leg of the flight. It is therefore encouraged to fly direct to keep costs down. Travelers must give up their tanks at the gate, use the tank supplied by the airline in-flight, and arrange to have an oxygen supplier meet them at their destination gate for a new tank. This process is very cumbersome to the traveler and requires much planning and organization.

Oxygen policies vary by airline, so it is strongly encouraged to check with the airline before traveling to ensure that they provide in-flight oxygen, and that they can supply the required flow rate. Airlines require a doctor's statement regarding the necessity for supplemental oxygen and a flow rate requirement before oxygen is administered.

Some airlines allow personal oxygen concentrators on board, while others will supply a concentrator if necessary. The *AirLife On-board Oxygen Concentrator* from AirSep Corporation is the first portable oxygen concentrator being considered by the FAA to be supplied by an airline and allowed as a carry-on. The *AirLife* is currently allowed on the aircraft, but only if supplied by the airline. This Notice of Proposed Rule Making (FAA-2004-18596) to make *AirLife* a carry-on was proposed on July 14, 2004, and is still in the process of being reviewed. If the rule is approved, similar portable oxygen generation devices may be approved, leading to much easier traveling experiences for oxygen users^{14, 15, 16}.

9.0 Conclusion

As in initial design, an oxygen concentrator achieving 95% oxygen purity was developed using pressure swing adsorption. Since this device design did not exceed the performance of other marketed products, a new device was developed for greater market advantage. The new design was a 99% oxygen tank filling device using pressure swing adsorption technology. To achieve 99% oxygen purity, another pressure swing apparatus was required in addition to nitrogen removal in order to remove the argon from the enriched oxygen stream. This device would be more economical than a home delivery system due to the elimination of monthly tank delivery costs. The PSA tank filler offers an immediately viable alternative for in-home oxygen therapy.

A portable ceramic oxide membrane device was also designed to give 5 lpm of 99% oxygen. The device weighs less than 18 lbs. and has a volume of approximately 2 ft³. The device can operate for 4 hours on direct current using a 12V lithium-ion battery. The membrane concentrator is the best option based on purity, portability, and economics. However, before the membrane oxygen device can be marketed, extensive research and testing must be carried out to ensure the safety and reliability of the device.

References

1. http://www.postgradmed.com/issues/1998/04_98/weg.htm
2. <http://health.discovery.com/encyclopedias/3015.html>
3. <http://www.a-msystems.com/pulmonary/nasalcannula/default.aspx>
4. http://www.walgreenshealth.com/whc/hcare/jsp/hc_patient_resp_services_provide_d_main.jsp
5. "Choosing Medical Insurance When You Have Chronic Lung Disease" California Thoracic Society, American Lung Association of California, 1999, rev. 2004.
6. <http://www.medicare.gov/Coverage/Search/Results.asp?State=OK%7COklahoma&Coverage=46%7COxygen+Therapy&submitState=View+Results+%3E>
7. <http://www.cchs.net/health/health-info/docs/2400/2412.asp?index=8707>
8. www.airsep.com
9. <http://www.airsep.com/medical/lifestyle.html>
10. <http://www.accessdata.fda.gov/scripts/cdrh/cfdocs/cfCFR/CFRSearch.cfm?fr=868.5440>
11. <http://www.fda.gov/cdrh/k863.html#overview>
12. <http://www.accessdata.fda.gov/scripts/cdrh/cfdocs/cfcfr/CFRSearch.cfm?CFRPart=807&showFR=1&subpartNode=21:8.0.1.1.5.5>

13. <http://www.fda.gov/cdrh/annual/fy2003/bringing.html>
14. http://www.tsa.gov/public/interapp/editorial/editorial_1568.xml
15. <http://www.homeoxygen.org/airtrav.html>
16. "Use of Certain Portable Oxygen Concentration Devices Onboard Aircraft: Proposed Rule" Part V, Department of Transportation, FAA, 14 CFR Parts 121, 125,135, *Federal Register*, vol. 69, no. 134, 14 July 2004.
17. Lababidi, H. M. S. "Air Separation by Polysulfone Hollow Fibre Membrane Permeators in Series," *Trans IChemE*, **2000**, 78, 1066.
18. Seader, J. D.; Henley, E. J. *Separation Process Principles*, John Wiley and Sons, New York, 1998, ch. 14.
19. Singhal, S.C.; Kendall, K. *High Temperature Solid Oxide Fuel Cells: Fundamentals, Design and Applications*, Elsevier, Oxford, UK, 2003, pp. 363
20. Ghosal, K.; Freeman, B. D. "Gas Separation Using Polymer Membranes: An Overview," *Polymers for Advanced Technologies*, **1994**, 5, 673.
21. Robeson, L.M. "Polymer Membranes for Gas Separation," *Current Opinion in Solid State and Materials Science*, **1999**, 4, 549.
22. Tan, X.; Li, K. "Modeling of Air Separation in a LSCF Hollow-Fiber Membrane Module," *AIChE Journal*, **2002**, 48, 1469.
23. http://www.airproducts.com/Products/Equipment/PrismGasGenerationSystems/Prism_nitrogen/permeation_intro.htm
24. http://www.pollutionengineering.com/CDA/ArticleInformation/features/BNP__Features__Item/0,6649,107618,00.html
25. <http://www.cheresources.com/hmembranes.shtml>
26. Goodenough, J. B. "Oxide-Ion Electrolytes," *Annu. Rev. Mater. Res.*, **2003**, 33, 91.
27. <http://www.wiretron.com/nicrdat.html>
28. <http://www.infraredheaters.com/metal.htm>
29. Kiehne, H. A. *Battery Technology Handbook*, 2nd ed., Marcel Dekker, Inc., New York, 2003, pp. 457-465.
30. Linden, D.; Reddy, T.B. *Handbook of Batteries*, 3rd ed., McGraw Hill, New York, 2002, pp. 22.12-22.13.
31. <http://aml.arizona.edu/classes/mse222/1998/perovskite/basicinfo.htm>
32. Biovin, J.C.; Pirovano, C.; Nowogrocki, G.; Mairesse, G.; Labrune, Ph.; Lagrange, G. "Electrode-electrode BIMEVOX System for Moderate Temperature Oxygen Separation," *Solid State Ionics*, **1998**, 113-115, 639.
33. Xia, C.; Lang, Y.; Meng, G. "Recent Advances to the Development of Low-Temperatures Solid Oxide Fuel Cells," *Fuel Cells*, **2004**, 4, 41.
34. Kleiner M.B; Kuehn S.A; Habberger K. "High Performance Air Cooling Scheme Using Ducted Microchannel Parallel Plate-Fin Heat Sinks," *Eleventh IEEE SEMI-THERM Symposium*, 1995, 122.
35. Perry R.H; Green D.W. *Perry's Chemical Engineers' Handbook*, 7th Ed., McGraw-Hill, New York, 1997.
36. <http://www.cotronics.com>
37. MSDS "Durabond 950" <http://www.msds.com>
38. <http://www.porextherm.com>
39. <http://www.thermalceramics.com>

40. Fenner, J. E., N. A. Dillon, M. Wong, "Ceramic Oxygen Generation System," US patent 6264807, 24 July 2001.
41. Hesselgreaves, J.E., *Compact Heat Exchangers*, Pergamon, Oxford UK, 2001, 139,158.
42. http://www.mcelwee.net/html/densities_of_various_materials.html
43. Kacmarek, R.M. "Delivery Systems for Long-Term Oxygen Therapy". *Respiratory Care*. Vol. 45. No. 1. January 2000. p. 84-94.
44. "Cryogenics". *Encyclopedia of Chemical Technology*. Ed: Kirk, R.E. 4th ed.
45. Arora, R., Dritz, T., Silva, L. "Microchannel Heat Exchangers Improve LNG Economics." *Gas-to-Liquids News*. March 2001. p. 7-8.
46. "AMISTCO Knitted Structured Packing". *AMISTCO Product Bulletin*. November 2003.
47. Phone price quote from Asco (Oklahoma City office) on Feb. 22nd 2005.
48. *Vacuum and Pressure Standard Product Catalog*. Rietschle Thomas. 2003. p. 6-9.
49. "SPI-ChemTM Molecular Sieve Type 13X".
http://www.2spi.com/catalog/spec_prep/molecular-sieve-type-13x.shtml
50. "Wheatland Schedule 40 Pipe". <http://www.wheatland.com/sch40.htm>
51. Santos, J.C., et. al. "Simulation and Optimization of Small Oxygen Pressure Swing Adsorption Units". *Industrial Engineering Chemical Res.* Vol. 43. November 26, 2004. p. 8328-8338.
52. Duong, D.D. *Adsorption Analysis: Equilibria and Kinetics*. p. 197.
53. Seader, J.D., Henley, E.J. *Separation Process Principles*. 1998. p. 832-843.
54. Auerbach, S.M., et. al. *Handbook of Zeolite Science and Technology*. p. 1066.
55. London Metal Exchange-Official Prices 3/10/2005. <http://www.metalprices.com>
56. American Metal Market. <http://www.amm.com>
57. Plumbing Supply.com. <http://www.plumbingsupply.com/copperpipe.html>
58. Phone price quote on Oxysiv 5 packing from Jack Corvini, UOP Adsorbents, Houston, TX. Feb 18th 2005.
59. Alliance Desiccants. http://www.biof.com/desiccants_silica.html
60. Action VW Enterprises. "Invacare 5".
<http://www.actionvw.com/Respiratorytherapy.htm>
61. "Altair Nanotechnologies Achieves Breakthrough in Battery Materials". Altair. Feb. 10, 2005.
<http://www.b2i.us/profiles/investor/ResLibrary.asp?BzID=546&ResLibraryID=8234&GoTopage=1&Category=24>
62. Linden, D., Reddy, T.B. *Handbook of Batteries*. 3rd edition. McGraw-Hill. 2002.
63. Alliance Desiccants. http://www.biof.com/desiccants_molsieve.html
64. Haraya, K.; Hwang, S.T. "Permeation of Oxygen, Argon, and Nitrogen through Polymer Membranes," *Journal of Membrane Science*, **1992**, 71, 13.
65. Knaebel, K.S.; Kandybin, A. "Pressure Swing Adsorption System to Purify Oxygen." US Patent 5,226,933. July 13, 1993.
66. Rege, S.U.; Yang, R.T. "Kinetic Separation of Oxygen and Argon Using Molecular Sieve Carbon." *Adsorption*. January 2000. Vol. 6. No. 1. pp. 15-22.
67. China CMS Net. http://www.chinacmsnet.com/CMSe/Products_e.htm

68. Robert's Oxygen. <http://www.robertsoxygen.com/R13RU/R13RU.htm>
69. Scuba.com,
http://scuba.com/shop/product.asp_category_155_categoryname_Compressors
70. Golden Hour Medical,
http://goldenhourmed.com/itemdetail-aluminum_oxygen_cylinders-b65.htm
71. Peters, M; Timmerhaus, K. *Plant Design and Economics for Chemical Engineers* 5th Ed, McGraw Hill, 2003.
72. MSDS "Resbond 907GF" <http://www.msds.com>
73. MSDS "Vacupor" <http://www.msds.com>

Supporting Materials

The following files can be found on the M: drive to support the PSA and cryogenic device sections:

- 95%economics.xls
- 99%economics.xls
- MembraneEconomics.xls
- Cryogenicproject.xls
- Final PSA costs, weight, and dimensions.xls
- Humidity levels.xls
- Polymer models argon.xls
- PSA modeling-Improved.xls
- Tank flow rate.xls
- Casing Drawing.vsd
- Components Drawing.vsd
- PFD.vsd
- 99%.out
- 99%.prz

The following files can be found on the M: drive to support the ceramic oxide membrane device section:

- Calc. for Capstone.xls
- Ceramic Oxide Membrane Separator with mixed conducting LSCF.xls
- Ionic Bicuvox and Power Calc final.xls
- Oxy proj worksheet.xls
- Users.xls
- Calculations.xls
- Copy of heat exchanger-Bicuvox-NEW.xls
- Microchannels.xls
- Polymer models.xls
- Final drawing of membrane casing (4 stacks).vsd
- Hx drawing.vsd

Appendix A1-Polymer Membranes Background

A1.1 Principles

Air separation using polymers membranes is limited by the partial pressure difference between the feed and permeate sides of the membrane. This study focuses on dense polymers because they exhibit higher selectivity than porous polymers. Selectivity refers to the ratio of the permeability of the faster component to that of the slower component. For the separation of oxygen from air, the permeate stream is enriched in oxygen, and the retentate stream is enriched in nitrogen. Similarly, the permeate stream is enriched in oxygen for the separation of oxygen and argon.

The mechanism of the dense polymer mass transport process is referred to as solution diffusion and is comprised of three main steps: solution of the permeating molecules on the feed side of the membrane, diffusion of the permeating molecules through the membrane to the low pressure side, and desorption from the membrane at the permeate side of the membrane. In general, the film mass-transfer resistances are assumed to be negligible compared to the resistance across the membrane. The permeability for polymer membranes, which follow the solution diffusion mechanism is given by the product of the component diffusivity in the membrane material and the solubility or Henry's law constant of the component¹⁸. The gas flux, N_A , through a polymer membrane is given by equation A1 with the driving force defined as

$$\text{polymer membrane driving force} = (p_{A,h} - p_{A,l}) \quad (\text{A1})$$

where p_A is the partial pressure of the gas, and the subscripts h and l refer to the high and low pressure sides of the membrane, respectively²⁰.

A1.2 Materials

The main classifications of polymers are crystalline, rubbery, and glassy. As mentioned earlier, crystalline porous polymers are not studied here due to their low selectivity for gas transport across the membrane. The rubbery and glassy polymers are

amorphous forms above and below the glass transition temperature of the polymer, respectively. In general, rubbery polymers exhibit lower selectivity than glassy polymers while glassy polymers have lower permeabilities values. These trends show that polymer material selection becomes a tradeoff between high permeability and high selectivity when designing a membrane device capable of producing high purity permeate and the required flow rate with a minimum area²⁰. Table A1 shows data for a number of polymers with reasonable values of permeability and selectivity for oxygen, nitrogen, and argon.^{21, 64}.

Table A1: Polymer Materials and Permeation Properties

type	material	permeability(cm ³ (STP) cm/ cm ² s cmHg)			selectivity		temperature (°C)
		oxygen	nitrogen	argon	O ₂ /N ₂	O ₂ /Ar	
glassy	polysulfone	1.20E-10	2.00E-11		6.00		35
glassy	polycarbonate	1.36E-10	1.82E-11		7.47		35
rubbery	silicone rubber	7.81E-08	3.51E-08		2.23		35
glassy	poly(4-methyl-1-pentyne)	2.70E-07	1.33E-07		2.03		25
glassy	trimethyleneperoxideazine- 4,4'-(Hexafluoroisopropylidene) diphthalic anhydride polyimide, (TMPA-6FDA)	1.22E-08	3.56E-09		3.43		35
glassy	poly(4-methyl-1-pentene), (PMP)	2.70E-09	6.70E-10		4.03		35
glassy	poly(trimethylsilylpropyne), (PTMSP)	9.71E-07	6.89E-07		1.41		25
glassy	poly(2,6-dimethyl-1,4-phenylene oxide), (PPO)	1.14E-09	3.50E-10	5.01E-10	3.26	2.28	35
glassy	tetramethyl bisphenol-A polycarbonate, (TMPC)	3.98E-10		1.64E-10		2.43	35

Appendix A2-Polymer Membrane Models

The hollow fiber membrane design has the highest surface area to volume ratio of the polymer membrane types; therefore, the performance of the membrane is better than other types which require more volume for the same separation. This membrane design is particularly important for devising a portable, compact device.

The flux of oxygen through polymer hollow fiber membranes can be modeled using the component and total mass balances over the total membrane. The streams of feed and permeate can flow in different combinations of directions: mixed flow, cross flow, co-current flow, counter-current flow. Figure A1 illustrates the arrangements of the streams for the flow modes. Each different arrangement is described by different forms of the mass balance equations. Because flow inside the tube side can be maintained at a higher pressure than the shell side, tube side feed is preferred.

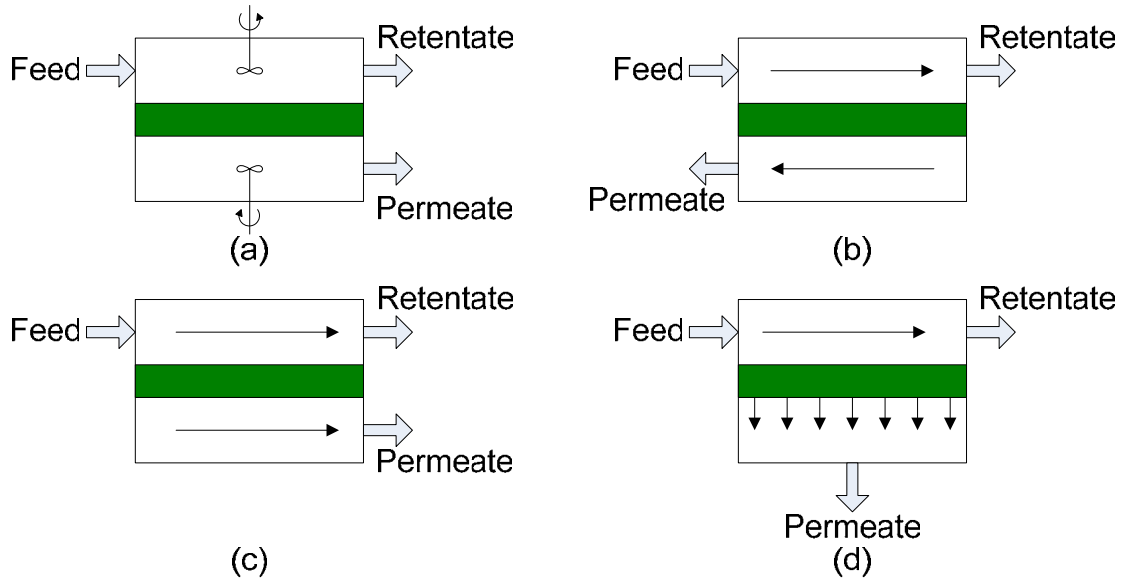


Figure A1: Membrane Flow Modes (a) mixed flow, (b) counter-current flow, (c) co-current flow, (d) cross flow

For the majority of the membranes studied, it is assumed that the feed stream is a binary gas composed of 79% nitrogen and 21% oxygen. The only exception is the polymer membranes designed to further purify the PSA product stream. They have feed streams with compositions of 95% oxygen and 5% argon. Polymer membrane models are based on the following assumptions: the membrane allows transport of both components according to their permeabilities, the effective membrane thickness is constant, the lengths of the hollow fibers are constant, bulk flow mass transfer dominates over diffusion along the flow path, plug flow (i.e. no axial dispersion of concentration) occurs for feed and permeate streams of co-current and counter-current models, the permeation operation is at steady state and is isothermal, there are no purge streams on the permeate side of the membrane, and the permeate stream is at atmospheric pressure¹⁷.

A2.1 Mixed Flow Polymer Model

A mixed flow membrane module consists of a membrane and two well-mixed chambers on either side of the membrane. This flow mode is not a realistic condition, but the calculations are useful for understanding the constant gradient case of polymer air separation. A feed stream on the high pressure side of the membrane loses a portion of its volume which passes through the membrane and becomes the permeate stream on the low pressure side. The concentration at any point on either side of the membrane is equal to the exit concentration on that side because of the mixing. Figure A2 shows the diagram for a mixed flow module labeled with the variables used in the model.

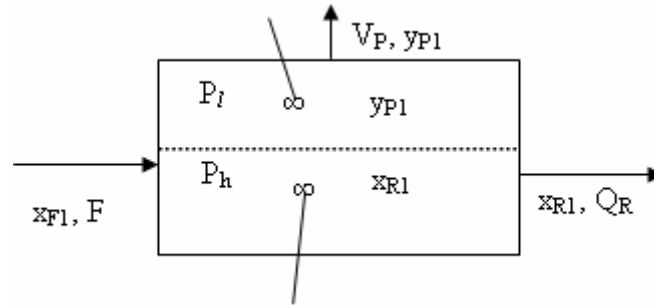


Figure A2: Mixed Flow Diagram

A model for this type of flow can be developed based on the following assumptions: the membrane allows transport of both components according to their permeabilities, the effective membrane thickness is constant, the lengths of the hollow fibers are constant, bulk flow mass transfer dominates over diffusion along the flow path, the permeation operation is at steady state and is isothermal, there are no purge streams on the permeate side of the membrane, and the permeate stream is at atmospheric pressure.

The model consists of component balances and membrane flux equations. The total volumetric flow rate balance for the entire module is

$$F = Q_R + V_P \quad (\text{A2})$$

where F is the feed flow rate, Q_R is the retentate flow rate, and V_P is the permeate flow rate.

The volumetric flow rate balance on oxygen (component 1) is

$$F x_{F1} = Q_R x_{R1} + V_P y_{P1} \quad (\text{A3})$$

where x and y are the compositions on the high and low pressure sides of the membrane, respectively, and the subscripts I , F , R , and P refer to component one, the feed stream, the retentate stream, and the permeate stream, respectively.

Volumetric flux through a polymer membrane is given by

$$N_i = \frac{R_i}{l} (P_h x_{Ri} - P_l y_{Pi}) = \frac{V_P y_{Pi}}{A} \quad (\text{A4})$$

where N is the flux, R is the permeance, l is the thickness of the membrane, A is the membrane area, P_h and P_l are the pressures on the feed and permeate pressures, respectively, and i is the component index where 1 is oxygen and 2 is nitrogen.

Plugging in for each component and remembering that the sum of the component fractions in a stream is equal to unity gives

$$V_P y_{P1} = A \frac{R_1}{l} (P_h x_{R1} - P_l y_{P1}) \quad (\text{A5})$$

and

$$V_P (1 - y_{P1}) = A \frac{R_2}{l} [P_h (1 - x_{R1}) - P_l (1 - y_{P1})]. \quad (\text{A6})$$

The equations can be simplified by introducing the following dimensionless parameters:

$$\alpha = \frac{AP_h}{F} (R_1 + R_2) \quad (\text{A7})$$

$$\pi = \frac{P_l}{P_h} \quad (\text{A8})$$

$$\gamma_1 = \frac{R_1}{R_1 + R_2} \quad (\text{A9})$$

$$\gamma_2 = \frac{R_2}{R_1 + R_2} \quad (\text{A10})$$

$$\theta_R^T = \frac{Q_R}{F} \quad (\text{A11})$$

$$\theta_P^T = \frac{V_P}{F}. \quad (\text{A12})$$

Equation A7 defines the dimensionless area (α), equation A8 defines the pressure ratio (π), equations A8 and A109 define the normalized permeabilities (γ_1 and γ_2), and equations A11 and A12 define the retentate and permeate flows (θ_R and θ_P).

By dividing equations A2, A3, A5, and A6 by F and equations A5 and A6 by P_h , the dimensionless forms of equations A2, A3, A5, and A6 are obtained as

$$1 = \theta_R^T + \theta_P^T, \quad (\text{A13})$$

$$x_{F1} = \theta_R^T x_{R1} + \theta_P^T y_{P1}, \quad (\text{A14})$$

$$\theta_P^T y_{P1} = \alpha \gamma_1 (x_{R1} - \pi y_{P1}), \quad (\text{A15})$$

and

$$\theta_P^T (1 - y_{P1}) = \alpha \gamma_2 [(1 - x_{R1}) - \pi (1 - y_{P1})], \quad (\text{A16})$$

respectively.

Adding equations A15 and A16 gives

$$\theta_P^T = \alpha \gamma_1 (x_{R1} - \pi y_{P1}) + \alpha \gamma_2 [(1 - x_{R1}) - \pi (1 - y_{P1})]. \quad (\text{A17})$$

Solving equations A13 and A14 for $\theta_P^T y_{P1}$ gives

$$\theta_P^T y_{P1} = \alpha \gamma_1 (x_{R1} - \pi y_{P1}) = x_{F1} - (1 - \theta_P^T) x_{R1}. \quad (\text{A18})$$

Equation A18 is rearranged for θ_P^T and combined with equation A16 to give

$$(x_{F1} - x_{R1}) = (1 - x_{R1}) \alpha \gamma_1 (x_{R1} - \pi y_{P1}) - x_{R1} \alpha \gamma_2 [(1 - x_{R1}) - \pi (1 - y_{P1})]. \quad (\text{A19})$$

The mole fraction of component 1 at any point in the permeate side is the ratio of the flux of component 1 to the sum of the fluxes of both components,

$$y_{P1} = \frac{\gamma_1 (x_{R1} - \pi y_{P1})}{\gamma_1 (x_{R1} - \pi y_{P1}) + \gamma_2 [(1 - x_{R1}) - \pi (1 - y_{P1})]}. \quad (\text{A20})$$

Mixed flow modeling involves four simultaneous nonlinear algebraic equations (A13, A14, A19, A20). Equations A19 and A20 are first solved for x_{R1} and y_{P1} . The nonlinear equations are solved simultaneously by guessing values for x_{R1} and y_{P1} and plugging the guesses into equations A19 and A20 rearranged with all terms on one side and zero on the other. The errors are defined as the differences between the calculated values with the guesses and zero. Minimizing the sum of the squares of the errors using Solver in Excel can be used to obtain the proper values for x_{R1} and y_{P1} . Then V_P and Q_R are determined from equations A13 and A14. This process can be repeated for different specified membrane areas and materials, feed compositions and flow rates, and pressures to yield different designs.

A2.2 Counter-Current Polymer Model

Counter-current flow has the largest driving force along the length of the membrane compared to the other flow modes. The driving force is quite strong with high feed pressure and atmospheric permeate pressure. Therefore, the counter-current flow with tube side feed is used for the polymer membrane design model rather than cross flow or co-current flow. Figure A3 shows the diagram for counter-current flow labeled with the variables used.

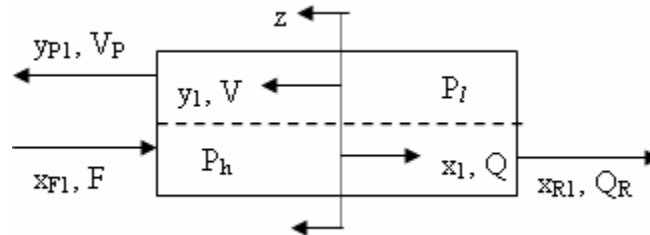


Figure A3: Counter-Current Flow Diagram

A counter-current flow membrane module consists of a membrane with a high pressure side and a low pressure side. A feed stream on the high pressure side of the membrane loses a portion of its volume which passes through the membrane and becomes the permeate stream traveling the opposite direction on the low pressure side. The concentration at any point on either side of the membrane is dependent on position along the membrane length since the driving force is different at each point. The total permeate composition is the average of the permeate compositions over the entire length of the membrane.

A model for this type of flow can be developed based on the following assumptions: the membrane allows transport of both components according to their permeabilities, the effective membrane thickness is constant, the lengths of the hollow fibers are constant, bulk flow mass transfer dominates over diffusion along the flow path, plug flow occurs on both sides of the membrane (i.e. there are no radial concentration gradients), the permeation operation is at steady state and is isothermal, there are no purge streams on the permeate side of the membrane, and the permeate stream is at atmospheric pressure.

The model consists of component balances and membrane flux equations. The total volumetric flow rate balance for any point z along the membrane length is

$$Q_R + V - Q = 0 \quad (\text{A21})$$

where Q_R , V , and Q are the flow rates of the total retentate, the local permeate, and the local retentate streams, respectively.

The volumetric flow rate balance on oxygen (component 1) at point z is

$$Q_R x_{R1} + V y_1 - Q x_1 = 0 \quad (\text{A22})$$

where x and y are the local compositions on the high and low pressure sides of the membrane, respectively, and the subscript l refers to oxygen.

The flux of the components changes along the membrane length. The differential equations for the fluxes of both components in the feed side to the permeate side are

$$\frac{d(Qx_1)}{dz} = AR_1(P_h x_1 - P_l y_1) \quad (\text{A23})$$

and

$$\frac{d(Q(1-x_1))}{dz} = AR_2[P_h(1-x_1) - P_l(1-y_1)]. \quad (\text{A24})$$

The variable z is set equal to zero at the feed end and equal to one at the exit end to allow integration from the exit to the feed. Because the z decreases in the direction of the feed flow, this makes the differential equations positive even though oxygen and nitrogen leave the feed stream.

The differential equations for the fluxes of both components in the permeate side from the feed side are

$$\frac{d(Vy_1)}{dz} = AR_1(P_h x_1 - P_l y_1) \quad (\text{A25})$$

and

$$\frac{d(V(1-y_1))}{dz} = AR_2[P_h(1-x_1) - P_l(1-y_1)]. \quad (\text{A26})$$

Equations A23 and A23 and equations A25 and A26 can be combined to give

$$Q \frac{dx_1}{dz} = (1-x_1)AR_1(P_h x_1 - P_l y_1) - x_1 AR_2[P_h(1-x_1) - P_l(1-y_1)] \quad (\text{A27})$$

and

$$V \frac{dy_1}{dz} = (1-y_1)AR_1(P_h x_1 - P_l y_1) - y_1 AR_2[P_h(1-x_1) - P_l(1-y_1)]. \quad (\text{A28})$$

Using the same dimensionless parameters defined previously, the dimensionless forms of equations A21, A22, A27, and A28 are

$$\theta_R^T + \theta_P - \theta_R = 0, \quad (\text{A29})$$

$$\theta_R^T x_{R1} + \theta_P y_1 - \theta_R x_1 = 0, \quad (\text{A30})$$

$$\theta_R \frac{dx_1}{dz} = (1 - x_1)\alpha\gamma_1(x_1 - y_1\pi) - x_1\alpha\gamma_2((1 - x_1) - \pi(1 - y_1)), \quad (\text{A31})$$

and

$$\theta_P \frac{dy_1}{dz} = (1 - y_1)\alpha\gamma_1(x_1 - \pi y_1) - y_1\alpha\gamma_2((1 - x_1) - \pi(1 - y_1)). \quad (\text{A32})$$

The mole fraction of component 1 at any point in the permeate side is the ratio of the local flux of component 1 to the sum of the fluxes of both components,

$$y = \frac{\gamma_1(x_1 - \pi y_1)}{\gamma_1(x_1 - \pi y_1) + \gamma_2((1 - x_1) - \pi(1 - y_1))}. \quad (\text{A33})$$

The counter-current model involves coupled, nonlinear ordinary differential equations. The boundary conditions of the equations are not completely known at either end because of the unknown permeate pressure inside the fibers. The boundary conditions that are known are listed below:

$$\text{At exit } z=0, x_1=x_{R1}, y_1 = y \text{ at } x_1=x_{R1}, \theta_R = \theta_R^T = \frac{Q_R}{F}, \theta_P = 0 \quad (\text{A34})$$

$$\text{At inlet } z=1, x_1=x_{F1}, y_1=y_{P1}, \theta_R = 1, \theta_P = \theta_P^T = \frac{V_P}{F} \quad (\text{A35})$$

The shooting method of numerical integration can be used to obtain a solution to the system of equations with incomplete boundary conditions. The method involves choosing an initial value for the unknown boundary condition at the exit side. The integration is performed with the finite difference method from the exit to the feed side. Solver in Excel is used to adjust the initial guesses to minimize the difference between the calculated inlet conditions and the actual inlet conditions. The inputs to the model (pressure, feed flow rate, membrane dimensions) can be changed to obtain designs which maximize the permeate composition or minimize the size of the membrane required to produce the desired flow rate.

A2.3 Cascade Model

An alternative to single membrane module is a cascade design in which the permeate stream of one module is fed to another module. Figure A4 illustrates an example of a membrane cascade designed to increase the concentration of the oxygen in the permeate stream. Cascades of polymer membranes can be modeled by changing the feed concentration and flow rate to match those values for the permeate stream calculated for the previous membrane design. Cascades could be useful for improving the concentration of the permeate stream; however, including another polymer membrane increases the size of the system. Additional modules may be added in parallel to modeled modules in order to achieve larger flow rates.

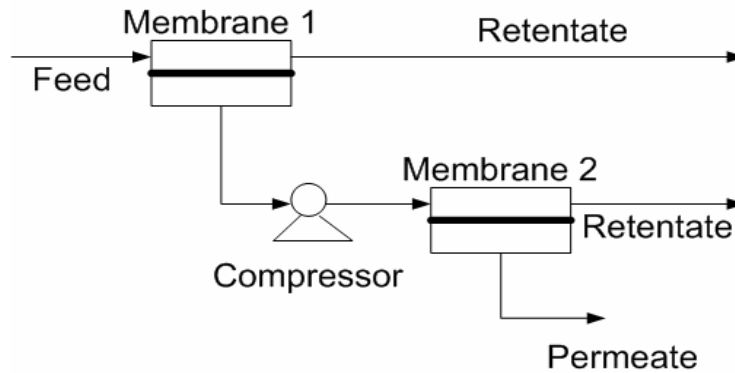


Figure A4: Cascade Flow Diagram

Appendix A3-Polymer Membrane Design Results

A3.1 Oxygen Separation from Air

The polymer mixed flow and counter-current models are used with different membrane materials, fiber dimensions, and number of fibers. The constraints on the design are the fiber bundle diameter (7.5 in based on the assumption of 50% of the total volume fraction occupied by the fibers) and length (12 in) and the permeate flow rate (5 lpm). Polycarbonate is the most selective of the membranes studied. With a 7.5 in. diameter module with 95,000 1 μm OD hollow fibers with an active fiber length of 10.2 in and inactive module length of 0.8 in on each side, this type of membrane can only produce a permeate stream with 53% oxygen for the mixed flow model and 36% oxygen

with the counter-current model. Other membranes with lower selectivity give lower concentrations of oxygen. The low concentration results from the low feed concentration of oxygen and the limited selectivity of the membrane for oxygen flux preferential to nitrogen flux.²⁰ The feed flow rate required to give 5 lpm of permeate for this design is 60 lpm. This flow rate can be reduced if concentration is decreased. So the design becomes a tradeoff between oxygen concentration of a particular membrane and the compressor size required to supply the feed.

Additionally, cascade designs are considered using the mixed flow model. Using the membrane discussed for the single mixed flow membrane design (7.5 in diameter, 10.2 in long, 53% oxygen, a composition of 84% oxygen can be obtained. However, seven parallel arrangements of these two-membrane cascades are required to give a permeate flow rate of 5 lpm. Obviously, this design is too large to be feasible for a portable device. The size of the membranes required can be reduced if the feed flow rate to the first stage is increased significantly. This adjustment would increase the compressor size required to supply the specified flow rate. This type of tradeoff must be considered when designing cascade arrangements.

A3.2 Removal of Argon from 95% Oxygen PSA Product Stream

The two polymers, TMPC and PPO, studied by Haraya and Hwang⁶⁴ which exhibit relatively high oxygen permeability and high selectivity between oxygen and argon are considered to further purify the product from the nitrogen selective PSA device. The operating pressures for the polymer membranes are 3 atm on the feed side and 1 atm on the permeate side. Pressure drop effects are neglected. This particular pressure differential is used because the polymer membranes were tested by Haraya and Hwang at this pressure difference. It is not known with certainty that the membranes would exhibit different behavior at larger pressure differentials nor that the membranes would be mechanically stable at significantly higher pressures.

For the models, it is assumed that thickness of membranes is approximately 40 microns with an inner diameter of roughly 40. These values are based on typical hollow fiber diameters values and the thickness of the polymer membranes used when the performance data was collected by Haraya and Hwang. Using a single membrane module, the highest permeate oxygen concentration is 97.35% using TMPC, the more

selective of the two membranes. The concentration is limited by the low partial pressure difference (both concentration and pressure differences are low) between the feed and the permeate stream. For a module with diameter of 7.48 in. and height of 10.24 in., 1300 lpm of feed are required to produce 5 lpm of oxygen product. The device size increases as the feed flow rate is decreased.

If a membrane could be found that had the same permeability as TMPC but had significantly higher selectivity for oxygen—around 7.75, then 99% purity could be obtained in a single module, but the flow rate considerations are still a factor because the permeability is not altered. For a reasonable feed flow rate of 15 lpm, the device should be 8.2 ft. in diameter and 3,281 ft. long which is approximately 2.5 times the height of the empire state building. These results show that the permeabilities and selectivities through the membrane seriously inhibit the use of polymer membranes for removing argon from air to produce 5 lpm of high purity oxygen.

In order to improve the design for this separation, it has been proposed to use a purge stream on the permeate side in order to increase the partial pressure difference between the two sides of the membrane. The counter-current model can be adjusted for this type of flow by defining the permeate composition at the exit side of counter-current rather than calculating it based on the retentate exit composition guess. Also, the total mass balances should be altered to consider the incoming purge stream. The purge stream requires another fan to flow the stream through the permeate stream. The use of a purge stream offers the advantage of decreasing the partial pressure on the permeate side which increases the driving force for flux across the membrane. Despite this advantage, it should not be used. The presence of a purge stream does not enhance the performance of the oxygen/argon separation because the purge is only useful if it is applied to the permeate stream when the retentate stream is the desired product. In this case, the oxygen permeate is the desired product. The problem of contamination of the permeate stream arises for the addition of a purge stream in this case. For instance, if some inert gas is used as the purge stream, another separation procedure is required to purify the permeate stream at the membrane exit. If air is used, then nitrogen is reintroduced into the oxygen product stream which defeats the purpose of the oxygen/nitrogen PSA process.

Cascades can be used to refine the design of the single permeator module. For two modules 10.24 in. long and 7.48 in. diameter each in series, the composition reaches 98.4%. The composition increases with each additional module in series. The main drawback of the cascade is that the size of the design increases significantly with the each series module. For the case mentioned above, the second module requires 20 lpm feed which is fed from the product streams of four of the modules before it. The total flow rate fed to those modules increases because there are now more of them. This increases the amount that needs to be produced by the PSA device, which greatly increases the size of the total design. Because of these size considerations and the slow increase in composition with each additional module, cascades do not solve the problems presented by using polymers membranes to remove argon from oxygen.

Appendix B1-Mixed Conducting Ceramic Oxide Membrane Background

B1.1 Principles

Ceramic oxide membranes are impervious to all gases at room temperature. At high temperatures, the concentration of oxygen vacancies in the internal lattice structure of the mixed conducting ceramic oxide increases to levels at which appreciable amounts of oxygen ions and electrons can permeate through the membrane at rates proportional to the partial pressure driving force. The main advantage of ceramic oxide membranes is their ability to allow the transport of oxygen only (i.e. no nitrogen flux through the membrane) which gives very high permeate purity (approximately 99% accounting for possible leaks). Mixed conducting membranes require no external electrical circuit.

The oxygen permeation mechanism is characterized by five steps which start at the high partial pressure side of the membrane: mass transfer of oxygen gas to the membrane surface, reaction between the molecular oxygen and the surface oxygen vacancies, oxygen vacancy bulk diffusion, reaction between lattice oxygen and electron-holes, and mass transfer of oxygen into the gas phase at the low partial pressure side of

the membrane²². The mass transfer resistances for the transfer of oxygen in the gas to and from the membrane surface are assumed to be negligible.

Ceramic oxide cells consist of a pair of porous electrodes which sandwich a nonporous electrolyte. Oxygen in air is reduced (gains electrons) at the cathode surface. Then the oxide ions (O^{2-}) are conducted through the electrolyte via vacancies in the crystal structure. On the other side of the electrolyte, the ions come in contact with the anode and oxidize to lose two electrons, reforming molecular oxygen.

B1.2 Materials

Mixed conducting ceramic oxides can be classified into four general types: $Sr(Co,Fe)O_{3-\delta}$ (SCF), $La(Co,Fe)O_{3-\delta}$ (LCF), $LaGaO_{3-\delta}$ (LGO), and nonperovskite oxides²². SCF, LCF, and LGO are all perovskites which is a class of ceramic oxides having structures favorable for the high temperature transport of oxygen ions through the material. Perovskites have of the general form ABO_3 where A is a cation with 2+ charge, B is cation with 4+ charge, and O is the oxygen ion, O^{2-} . The A and B components can be a number of combinations of rare earth, alkaline earth, and inner transition metals. The typical perovskites structure is a face centered cubic lattice with O atoms on the faces, A atoms at the corners, and the B atom occupying the center of the lattice. This structure is prone to forming electric dipoles and oxygen vacancies at high temperatures and under imposed gradients³¹. Because of its high oxygen permeability and good chemical stability, $La_{0.6}Sr_{0.4}Co_{0.2}F_{0.8}O_{3-\delta}$ (LSCF) was chosen for the mixed ceramic oxide material.

Appendix B2-Mixed Conducting Ceramic Oxide Model

Since mixed conducting ceramic membranes are driven by the partial pressure difference, the membrane design considerations are similar to those given for polymer membranes. The hollow fiber is chosen as the membrane design due to the need for high surface area to volume ratios and maximum partial pressure differentials along the membrane. The mixed conducting ceramic oxide model employs the same assumptions as the polymer model with the following exceptions: the membrane is impermeable to

nitrogen, and the transport fluxes of charged defects are only in the radial direction not the axial direction.

Despite the similarities, the mixed conducting membranes require a different model than the polymer membranes due to the facts that only oxygen is transported across the membranes and that the oxygen permeability through the membranes does not merely depend on the diffusivity and Henry's Law constants. The mixed conducting model considers the oxidation/reduction reactions at the membrane surfaces and the diffusion through the membrane rather than the solutions diffusion mechanism used for the polymer membrane models.

Oxygen ion transport across mixed conducting ceramic oxide membranes can be modeled by a mechanism involving the reaction between the molecular oxygen and the surface oxygen vacancies, oxygen vacancy bulk diffusion, and the reaction between lattice oxygen and electron-holes.

The reactions between oxygen and the surface oxygen vacancies and between lattice oxygen and electron-holes are modeled as



and



respectively, where O_O^x is the lattice oxygen in the crystal structure, h is the electron hole concentration, and V_O is the oxygen vacancy. Equation B1 describes the local rate of oxygen consumed in the reaction between the molecular oxygen and the surface oxygen vacancies. Equation B2 describes the local rate of oxygen formed by the reaction between lattice oxygen and electron-holes reaction between lattice oxygen and electron-holes.

The kinetics rate expressions corresponding to the reactions in equations B1 and B2 are

$$dN_{O_2} = 2\pi R_o [k_f (p_{O_2}')^{0.5} C_V' - k_r] dl \quad (B3)$$

and

$$dN_{O_2} = 2\pi R_i [k_f - k_r (p_{O_2}'')^{0.5} C_V''] dl, \quad (B4)$$

respectively, where N_{O_2} is the molar flow rate of oxygen; R_o and R_i are the outer and inner radii of the hollow fiber, respectively; k_f and k_r are the forward and reverse reaction rates of the surface reactions, respectively; p_{O_2}' and p_{O_2}'' are the partial pressures of oxygen at the hollow fiber membrane outer and inner surfaces, respectively; and C_V' and C_V'' are the concentrations of oxygen vacancies on the outer and inner surfaces of the membrane.

The local oxygen molar flow rate for the oxygen vacancy bulk diffusion is given by

$$dN_{O_2} = \pi D_V \frac{C_V'' - C_V'}{\ln \frac{R_o}{R_i}} dl \quad (B5)$$

where D_V is the oxygen vacancy diffusivity, the difference in oxygen vacancy concentrations is the driving force, and the other terms are characteristic for the membrane tubular geometry.

By adding equations B3, B4, and B5 in a manner similar to resistors in parallel, the relationship between the local oxygen permeate rate in a hollow fiber and the partial pressure of oxygen can be obtained.

$$dN_{O_2} = \frac{k_r [(p_{O_2}')^{0.5} - (p_{O_2}'')^{0.5}]}{\frac{k_f \ln(R_o / R_i) (p_{O_2}'')^{0.5}}{\pi D_V} + \frac{(p_{O_2}')^{0.5}}{2\pi R_i} + \frac{(p_{O_2}'')^{0.5}}{2\pi R_o}} dl \quad (B6)$$

The mixed conducting model can be used for different inputs of fiber inner and outer diameter and length, feed composition and flow rate, partial pressures, and rate constants. The rate constants used for the model were determined experimentally by Tan²² for LSCF. The model uses finite difference to integrate B6 along the length of the hollow fiber tubes. The flux gives the rate of oxygen transport across the membrane which is the permeate flow rate. Varying the inputs allows for the design of membrane devices that meet different specifications. Example uses include determining the smallest size device that can be used to obtain the desired permeate flow rate and composition or the separating performance of a membrane of a specified size.

Appendix B3-Design Results for Mixed Conducting Ceramic Oxide Membranes

The model equations were solved by Tan and Li for LSCF hollow fibers for both counter-current and co-current flow modes with the conditions listed in Table B1. The results of that study give higher oxygen permeation fluxes for co-current mode so that mode is chosen for the calculations. At a feed pressure of 1 atm and vacuum pressure of 0.01 atm, the oxygen permeate flux is $0.00225 \text{ mol m}^{-2} \text{ s}^{-1}$ and the oxygen recovery from the feed is 95%.

For a length of 12 in, module diameter of 7 in, and 178 fibers, the area is 228 cm^2 . The oxygen flux rate is used to calculate the oxygen flow rate of 0.0689 lpm. This result indicates that a small scale device does not produce sufficient oxygen flow rates. Other geometries and pressures should be considered in the future in order to verify this conclusion.

Table B1: Parameters and Values for LSCF Mixed Conducting Ceramic Membrane Calculations

Parameter	Value		
OD of the hollow fiber	d_o	0.1	cm
ID of the hollow fiber	d_i	0.05	cm
Vacuum pressure in tube side of fiber	P_v	0.01	atm
Pressure on shell side of fiber	P	1	atm
Operating temperature	T	1273	K
Oxygen productivity	α	0.95	
Oxygen permeate flux	q	0.00225	$\text{mol m}^{-2} \text{ s}^{-1}$
Diffusion coefficient of oxygen vacancy	D_v	1.509E-05	$\text{cm}^2 \text{ s}^{-1}$
Forward reaction rate constant	k_f	0.002886	$\text{cm atm}^{-0.5} \text{ s}^{-1}$
Reverse reaction rate constant	k_r	2.597E-06	$\text{cm atm}^{-0.5} \text{ s}^{-1}$

Appendix C-Calculations for Determining the Cold Face Temperature of the Vacuum Insulation Panels

The cool face of the vacuum insulation was calculated using the Fourier equation for heat transfer through conduction, and Newton's rate law for cooling.

$$\frac{q_x}{A} = -k \left(\frac{dT}{dx} \right) \quad (C1)$$

$$\frac{q}{A} = h\Delta T \quad (C2)$$

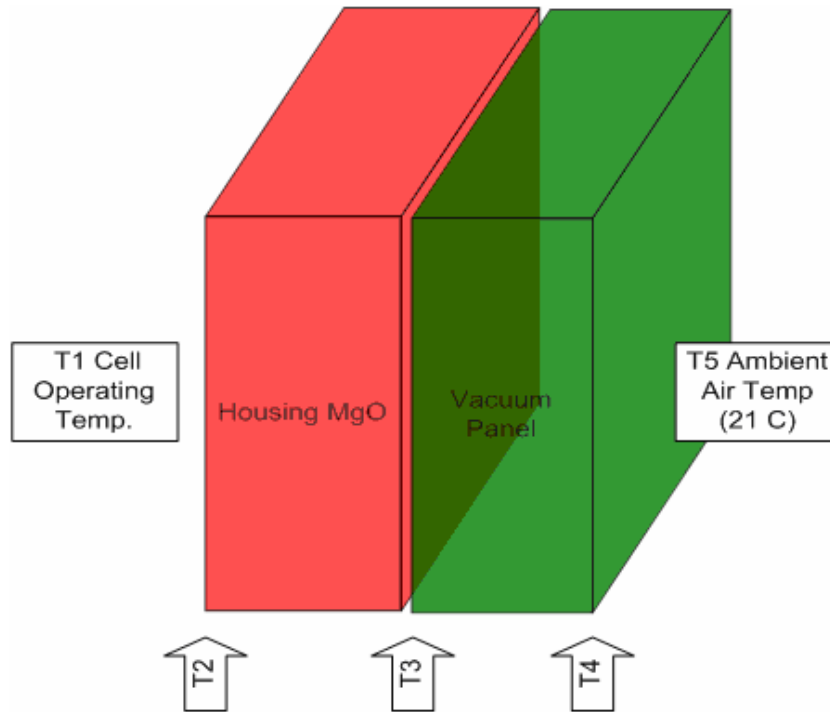


Figure C1: Heat Transfer Schematic of Insulation and Housing

There are two known temperatures, T_1 and T_5 . T_2 through T_4 are unknown. T_1 is the temperature of the air in the cell stack, which is the cell operating temperature. T_2 is the temperature at the air/housing interface. T_3 is the temperature on the interface between the MgO housing and vacuum panel. T_4 is the temperature on the outside of the vacuum panel, the cold face temperature to be solved for. T_5 is the temperature of the ambient air; room temperature, 293K. Writing equations for each air to solid, and solid thickness, and summing, results in the following equation:

$$q = \frac{T_1 - T_5}{\left[\left(\frac{x_{MgO}}{A \cdot k_{MgO}} \right) + \left(\frac{x_{vac}}{A \cdot k_{vac}} \right) + \left(\frac{2}{h_{air}} \right) \right]} \quad (C3)$$

Using a k value for MgO of 30 W/mK, a k for the vacuum panels of 0.0048 W/mK, an air h value of 5 W/mK, an MgO housing thickness of 0.5 cm, and a vacuum panel thickness of 7.5 cm, the q value was found to be 35.26 W. The vacuum panel thickness was found using solver to produce the desired cold face temperature. Solving the temperature equations for T_4 in terms of q, a cold face temperature of 27.1°C (80.7°F) is found.

Appendix D-Double Pipe Heat Exchanger Design

The dimensions of the double-pipe heat exchanger were calculated using convective heat transfer correlations for laminar flow found in Perry's Chemical Engineers' Handbook³⁵. The Nusselt number correlation for laminar flow in tubes is a function of the Graetz number, Gz. The Graetz number is also a function of the Reynolds and Prantel numbers, as well as length. The Graetz number and Nusselt number correlations are given below.

$$Gz = \frac{Re \ Pr \ D}{L} \quad (D1)$$

$$Nu = 3.66 + \frac{0.19Gz^{0.8}}{1 + 0.117Gz^{0.467}} \quad (D2)$$

The convective heat transfer coefficient, h, was then calculated as a function of the length down the exchanger using the following correlation.

$$h = \frac{kNu}{D} \quad (D3)$$

Finally, the overall heat transfer coefficient, U , and the change in air temperature with length through the tubes were calculated using the relationships below. To simplify the calculation of U , it was assumed that the tubes are thin-walled, resulting in the equivalence of the inner and outer surface areas. This results in the U correlation for cylindrical geometry given below.

$$\frac{1}{U} = \frac{1}{h_i} + \frac{r_o - r_i}{k} + \frac{1}{h_o} \quad (\text{D4})$$

$$\frac{dT}{dx} = \frac{UA\Delta T}{\sum mC_p} \quad (\text{D5})$$

Since the feed air stream must be split proportionally to effectively cool the exiting oxygen and lean air streams, there is a need for two double-pipe exchangers. Therefore, the above procedure was performed twice: once for the air-oxygen streams and once for the air-nitrogen streams. To conserve space, the two pipe sections were coiled tightly while still achieving the necessary pipe lengths. The schematic of this heat exchanger design can be seen in Figure D1.

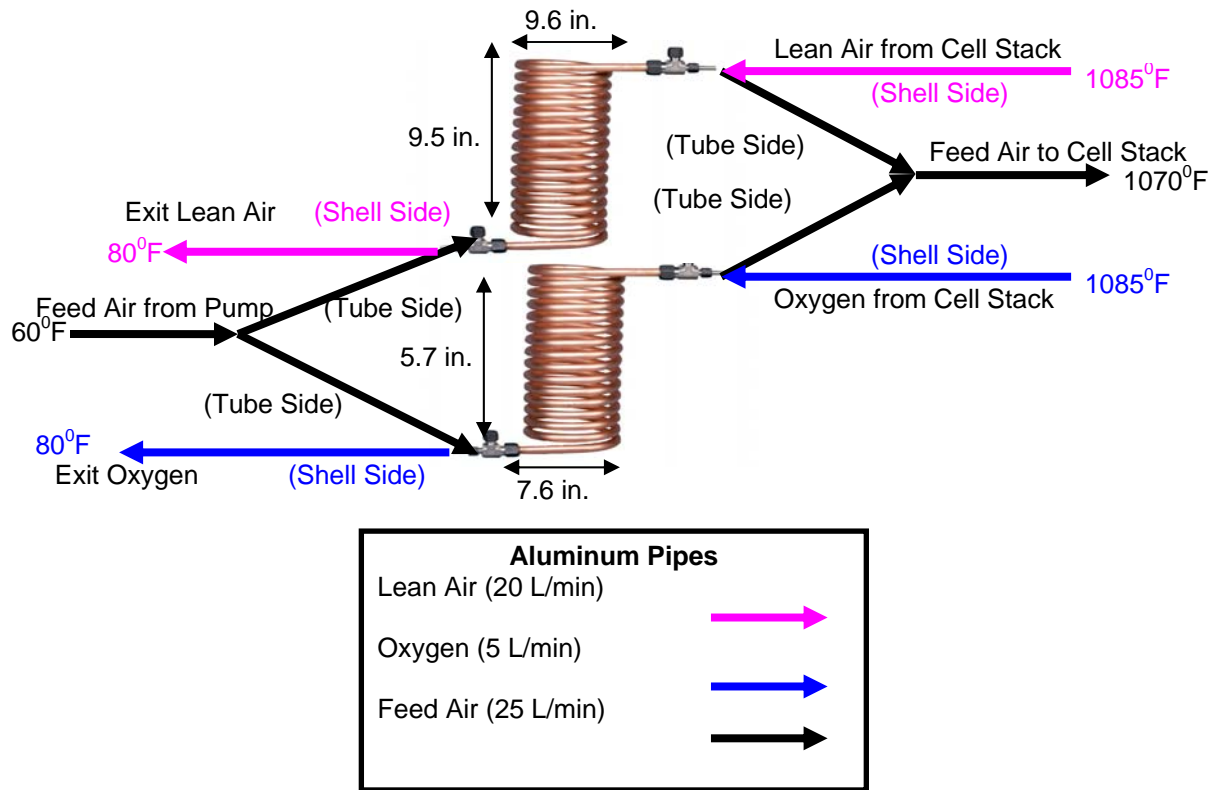


Figure D1: Double-Pipe Heat Exchanger Design

Appendix E-Cryogenic Oxygen Separation

E.1 Introduction and Theory

Concepts for the cryogenic separation of air were developed in the late 19th and early 20th century and a double distillation column to produce nearly pure oxygen was developed by Carl von Linde in 1905. For conventional cryogenic systems, atmospheric air is compressed to between 5 and 8 atmospheres and then cooled to nearly ambient temperatures with an aftercooler. For large volumes of compressed air, the cooling is done with a heat exchanger using water as the cooling fluid. For systems with relatively low air flowrates, sufficient cooling can be done by attaching fins to the compressed air pipe and positioning a fan to remove the heat from the compressed stream. After the air is cooled, adsorbents are used to remove all water, carbon dioxide, and trace

hydrocarbons. Water and carbon dioxide must be removed because they exist in the solid phase at the column operating temperatures. Trace organic volatiles and other airborne particles, such as dust, must also be removed to prevent accumulation in the distillation column. After the air is reduced to the three primary components of 78% nitrogen, 21% oxygen, and 1% argon, the air is passed through a cold temperature heat exchanger, or coldbox. The cold-side fluids in the coldbox are the streams leaving the distillation column which are heated to near ambient temperatures while cooling the entering air to cryogenic temperatures.⁴⁴

A small portion of the air stream is diverted prior to entering the coldbox where it is further compressed and cooled by a separate aftercooler before it too passes through the coldbox. After leaving the coldbox, the smaller air stream is expanded to atmospheric pressure and passed through the condenser. If designed correctly, this stream provides all the cooling energy required by the distillation column. Once this stream has cooled the condenser, its energy is recovered by passing it through the coldbox on the cold side.⁴⁴

The primary air stream is cooled in the coldbox to near its condensation temperature. This stream first goes to the high pressure section of the distillation column. The high pressure section separates the entering air into nitrogen and oxygen rich stream that passes to the upper low pressure column. The low pressure column produces nearly pure oxygen from the bottoms product. The top stream is nearly pure nitrogen and it also contains most of the argon that was initially in the feed. Both the oxygen product and nitrogen waste streams pass through the coldbox to recover their energy and bring the oxygen to a safe temperature for breathing.⁴⁴ Figure E.1 shows the cryogenic distillation flow diagram.

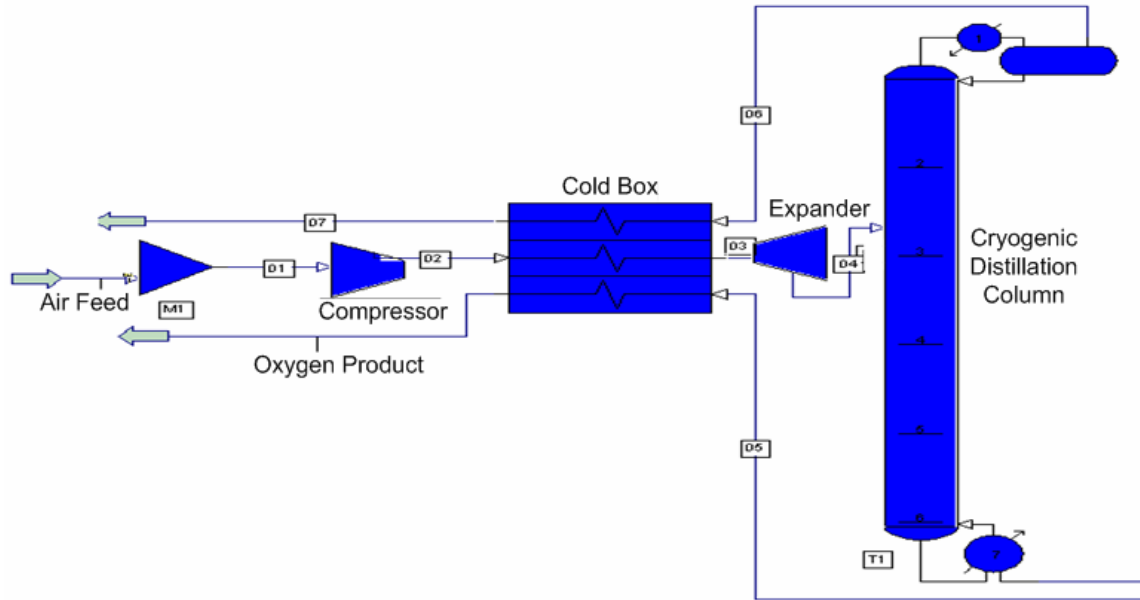


Figure E.1 Cryogenic Distillation Flow Diagram

E.2 Structured Distillation Column

There are several advantages of using a column with structured packing as compared to using a series of flash tank. One advantage is the increase in stage efficiency causing a greater separation at each theoretical stage of the column and resulting in higher purity. Structured packing was chosen over trays for the internals of the column in order to reduce the height of the column. Another advantage is that there is less surface area to insulate which results in a more energy efficient system.

The column is designed to have 7 height equivalent theoretical stages. In order to lower the height of the column structured packing was used with a height equivalent to a theoretical plate of 4 inches⁴⁶ resulting in a final column height of 2 feet 4 inches. The width of the column was calculated based on the superficial vapor velocity. A width of 6 inches caused a superficial vapor velocity of 0.64 ft/s. In order to make sure that this width would not cause flooding, a prototype column should be built and tested at various flow-rates to find when flooding started.

Air at ambient temperatures will be used to provide heat for the heat exchanger that is serving as a boiler. In this process the boiler and the condenser do not serve as separation stages so all seven stages are accounted for in the column itself.

E.3 Series of Flash Tanks vs. Distillation Column

In order to intensify the cryogenic oxygen separation process, modifications may be made to the traditional design of a cryogenic separation plant. Due to the dimensional constraints of a distillation column, a series of flashes may be used instead. The advantage of using flashes is that the design is not constrained to be a rigid vertical structure. However, to allow the liquid from a higher flash container to flow to the container below, the bottom of the higher container must be at the height of the liquid in lower container. Since the height of liquid in each flash container is set to be one half the height of the column, the total height of the series of flashes is equal to one half of the sum of the heights of all the flash containers. The disadvantage of using a series of flashes is that the total volume of the flashes is larger than the volume of an equivalent distillation column. A portion of the decreased efficiency results from a large surface area of flash containers that must be insulated.

Table E.1 shows the results from a Pro/II simulation (simulation 99%.prz) that was obtained from a distillation column. Using the liquid flow rates in each tray, flash containers were sized assuming a liquid retention time of 30 seconds per flash container. 30 seconds was chosen as an appropriate retention time due to the low liquid and vapor flowrates found in Pro/II simulations. The duties of the reboiler, condenser, reflux ratio, product purity, product flow rate, and compressor work are also listed. The simulation results indicate that a series of flashes can be used to produce a 5.4 L/min stream of 99% pure oxygen. The largest volume of a flash container is approximately 20 in³. Assuming the flash container height is twice the diameter, the largest flash container is about 5 inches.

Table E1: Flash Simulation Specifications

Distillation column							
7 trays (chosen for limited volume availability): tray 1 is a condenser and tray 7 is a reboiler							
optimum feed is between trays 2 and 3							
Performance:				tray temp (F)	Duty (MMBtu/hr)		
inlet flow (l/min)	35		1	-312.2	-0.003342		
Purity%	98.96		2	-308.1			
Recovery	0.7347		3	-302			
Product (l/min)	5.457		4	-296			
Bottoms (l/min)	29.543		5	-293.1			
Reflux ratio	8		6	-292.2			
Optimum feed tray	2.7		7	-291.9	0.003391		
O ₂ available (l/min)	7.35						
Column P (psia)	20						
Compressor work (hp)	0.2142						
Retention time (min)	0.5						
tank h/D (in)	2						
Tray	1	2	3	4	5	6	7
liquid volume throughput ft ³ /hr	0.71200	0.65400	0.60800	0.57100	0.55600	0.54900	0.01400
V (ft ³)	0.00593	0.00545	0.00507	0.00476	0.00463	0.00458	0.00012
V _{tank} (ft ³)	0.01187	0.01090	0.01013	0.00952	0.00927	0.00915	0.00023
V _{tank} (in ³)	20.50560	18.83520	17.51040	16.44480	16.01280	15.81120	0.40320
h (in)	4.70920	4.57769	4.46775	4.37522	4.33656	4.31829	1.27105
D (in)	2.35460	2.28885	2.23387	2.18761	2.16828	2.15914	0.63553

E.4 Modified Oxygen Generation Process

Figure E.2 shows a system of seven flash containers used for oxygen separation. In the diagram, everything to the right of the heat exchanger located in the center of the diagram, is enclosed in a vacuum insulated compartment. The heat exchangers used are microfluidic heat exchangers that have approximately ten times the heat transfer rate of traditional heat exchangers due to the increase in surface area per relative fluid flowrate.⁴⁵

The sequence begins by compressing 35-40 L/min of air to about seven atmospheres followed by finned pipes that cool the compressed stream to near ambient temperatures. After cooling, a molecular sieve removes water vapor, carbon dioxide, and

trace hydrocarbons. From the cleaned air stream, a small portion of the air is further compressed and cooled by another compressor and aftercooling process. The purpose of this side stream is to later provide the duty to the condenser. The two air streams then pass through a microchannel heat exchanger where they are cooled to near the dew point of air. After exiting the heat exchanger, the primary feed stream is passed through an expander to about 1.5 atmospheres where it enters the third flash container as a mixture of vapor and liquid. The side stream is passed through a separate expander where it is expanded to one atmosphere and passes through a microfluidic heat exchanger that acts as a condenser for the vapor exiting the top flash container. From the bottom flash container, a portion of the heavy liquids is reboiled by flowing the fluid through a pipe outside the vacuum insulated compartment where heat is added from the atmosphere. Once the desired purity of oxygen in the bottoms is achieved, the oxygen stream and the waste nitrogen stream pass through the primary microfluidic heat exchanger where they are heated to ambient temperatures while their energy is recovered by cooling the entering air.

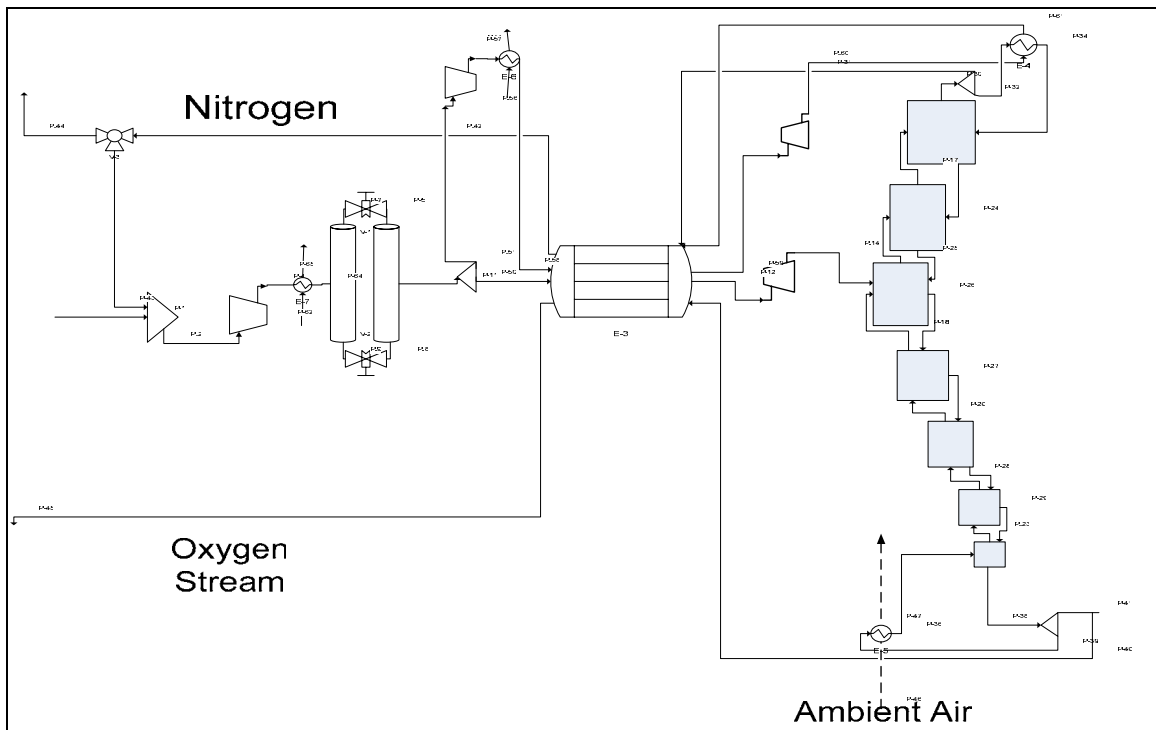


Figure E.2 Modified Oxygen Generation Process Flow Diagram

E.5 Cost Evaluation

The costs of the components needed to build the flash device and the packed column are outlined in Table E.2. The total cost for the series of flash tanks is \$13,660 and the cost for the packed column is \$12,040.

Table E.2 Cost of Flash and Packed Column Components

Flash			Packed Column		
Component	# of units	Price/unit	Component	# of units	Price/unit
Solenoid Valves ⁴⁷	3	\$81	Solenoid Valves ⁴⁷	3	\$81
Compressors ⁴⁸	2	\$500	Compressor ⁴⁸	2	\$500
Mixer/Splitter	4	\$50	Mixer/Splitter	4	\$50
Primary Heat Exchanger	1	\$3,000	Primary Heat Exchanger	1	\$3,000
Condenser Heat Exchanger	1	\$2,000	Condenser Heat Exchanger	1	\$2,000
Air Purification System Hardware	1	\$100	Air Purification System Hardware	1	\$100
Molecular Sieve ⁴⁹	2731g	\$3,520	Molecular Sieve ⁴⁹	2731g	\$3,520
Piping and Fittings		\$500	Piping and Fittings		\$500
Custom Vacuum Insulation		\$1,000	Custom Vacuum Insulation		\$1,000
Dewar (flash vessels)	7	\$300	Packed Column ⁵⁰		\$175
			Packing ⁴⁶		\$300

E.6 Cryogenic Technology Summary

Two viable designs exist to cryogenically produce oxygen from air: a series of flash columns (flash design) or a miniature distillation column (structured column design). Current simulations show the structured column design to be less expensive, smaller, and easier to insulate than the flash design.

The advantage of cryogenically separating oxygen from air is the high purity that can be achieved. Another advantage is the high recovery of oxygen compared to other separation devices. Compared to other in-home devices, the 99% purity achieved in the Pro/II simulations has almost no competition. The disadvantages of the cryogenic oxygen separation devices are low energy efficiency, device weight, and several safety

concerns such as low temperature operation. The most significant drawback to this technology is the device cost.

Appendix F- NPW, TCI Calculations and Happiness Graphs

Ceramic Membrane Device

Table F.1 TCI and FCI Calculation for Ceramic Membrane Device

Capital Investment for Portable Oxygen Device		
	Percent of Equipment Cost	
Direct Costs		
Purchased equipment delivered	100	\$30,000,000
Purchased-equipment installation	45	\$13,500,000
Instrumentation and controls	18	\$5,400,000
Piping	16	\$4,800,000
Electrical systems	10	\$3,000,000
Buildings	25	\$7,500,000
Yard Improvements	15	\$4,500,000
Service facilities	40	\$12,000,000
Total direct plant cost	269	\$80,700,000
Indirect costs		
Engineering and supervision	33	\$9,900,000
Construction expenses	39	\$11,700,000
Legal expenses	4	\$1,200,000
Contractor's fee	17	\$5,100,000
Contingency	35	\$10,500,000
Total indirect plant cost	128	\$38,400,000
Fixed Capital Investment	397	\$119,100,000
Working Capital (15% of TCI)	70	\$21,017,647
Total Capital Investment	467	\$140,117,647

Table F.2 NPW Calculation for Ceramic Membrane Device

Year,n	Demand	Sales (\$/year)	Product Cost	Gross Earnings	Depreciation	Taxes	Net Profit	Cash Flow	CFn/((1+r)^n)
1	9	1.E+05	2.E+07	-2.E+07	1.E+07	4.E+03	-3.E+07	-2.E+07	-2.E+07
2	5,206	7.E+07	3.E+07	3.E+07	1.E+07	2.E+06	2.E+07	3.E+07	2.E+07
3	7,465	9.E+07	4.E+07	5.E+07	1.E+07	3.E+06	4.E+07	5.E+07	4.E+07
4	8,751	1.E+08	4.E+07	7.E+07	1.E+07	4.E+06	5.E+07	6.E+07	4.E+07
5	9,584	1.E+08	5.E+07	7.E+07	1.E+07	4.E+06	6.E+07	7.E+07	4.E+07
6	10,167	1.E+08	5.E+07	8.E+07	1.E+07	4.E+06	7.E+07	7.E+07	4.E+07
7	10,599	1.E+08	5.E+07	8.E+07	1.E+07	5.E+06	7.E+07	8.E+07	4.E+07
8	10,932	1.E+08	5.E+07	9.E+07	1.E+07	5.E+06	7.E+07	8.E+07	4.E+07
9	11,195	1.E+08	5.E+07	9.E+07	1.E+07	5.E+06	8.E+07	8.E+07	4.E+07
10	11,410	1.E+08	5.E+07	9.E+07	1.E+07	5.E+06	8.E+07	9.E+07	3.E+07
								NPW	\$166,867,738

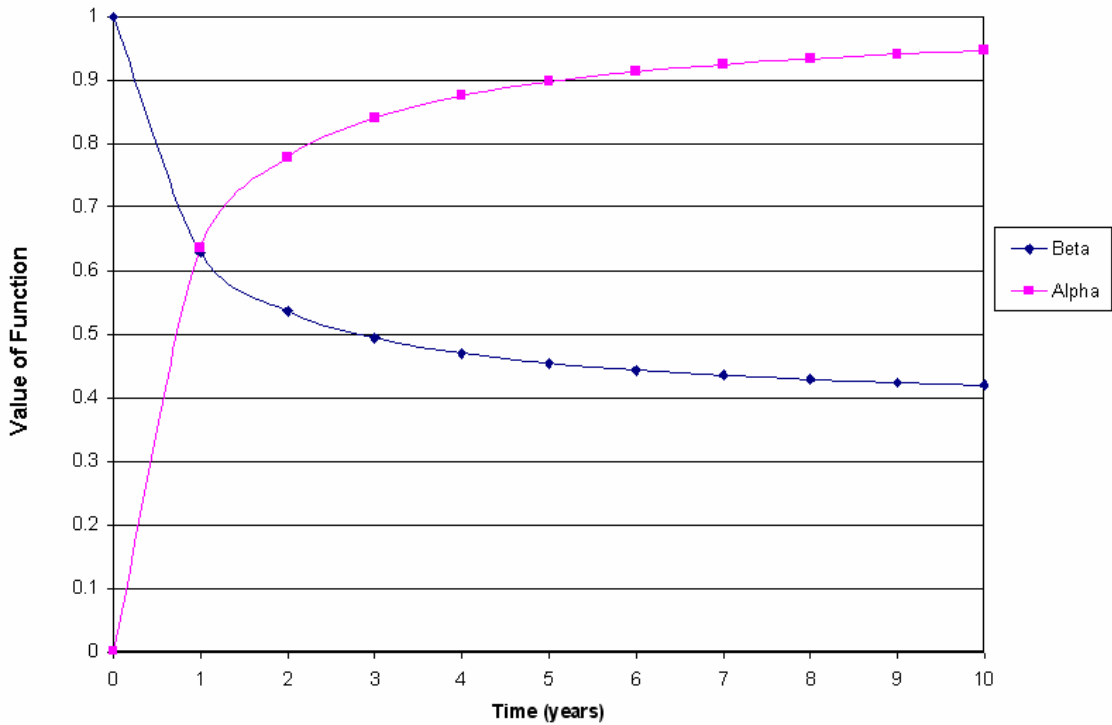


Figure F.1 Alpha and Beta Function vs. Time for Ceramic Membrane Device

95% Oxygen Device

Table F.3 NPW Calculation for Ceramic Membrane Device

Capital Investment for Portable Oxygen Device		
Direct Costs	Percent of Equipment Cost	
Purchased equipment delivered	100	\$1,018,412
Purchased-equipment installation	45	\$458,285
Instrumentation and controls	18	\$183,314
Piping	16	\$162,946
Electrical systems	10	\$101,841
Buildings	25	\$254,603
Yard Improvements	15	\$152,762
Service facilities	40	\$407,365
Total direct plant cost	269	\$2,739,528
Indirect costs		
Engineering and supervision	33	\$336,076
Construction expenses	39	\$397,181
Legal expenses	4	\$40,736
Contractor's fee	17	\$173,130
Contingency	35	\$356,444
Total indirect plant cost	128	\$1,303,567
Fixed Capital Investment	397	\$4,043,095
Working Capital (15% of TCI)	70	\$713,487
Total Capital Investment	467	\$4,756,582

Table F.4 NPW Calculations for 95% Oxygen Concentrator

Year,n	Demand	Sales (\$/year)	Product Cost	Gross Earnings	Depreciation	Taxes	Net Profit	Cash Flow	CFn/((1+r)^n)
1	2	3.E+03	3.E+04	-3.E+04	2.E+04	1.E+02	-5.E+04	-3.E+04	-3.E+04
2	1,004	2.E+06	1.E+06	4.E+05	2.E+04	6.E+04	3.E+05	3.E+05	3.E+05
3	1,409	2.E+06	2.E+06	5.E+05	2.E+04	8.E+04	5.E+05	4.E+05	3.E+05
4	1,633	3.E+06	2.E+06	6.E+05	2.E+04	9.E+04	6.E+05	5.E+05	4.E+05
5	1,774	3.E+06	2.E+06	7.E+05	2.E+04	1.E+05	6.E+05	6.E+05	4.E+05
6	1,872	3.E+06	2.E+06	7.E+05	2.E+04	1.E+05	7.E+05	6.E+05	3.E+05
7	1,944	3.E+06	2.E+06	7.E+05	2.E+04	1.E+05	7.E+05	6.E+05	3.E+05
8	1,999	3.E+06	2.E+06	8.E+05	2.E+04	1.E+05	7.E+05	6.E+05	3.E+05
9	2,042	3.E+06	3.E+06	8.E+05	2.E+04	1.E+05	7.E+05	7.E+05	3.E+05
10	2,077	3.E+06	3.E+06	8.E+05	2.E+04	1.E+05	8.E+05	7.E+05	3.E+05
								Net Present Worth	\$2,361,527

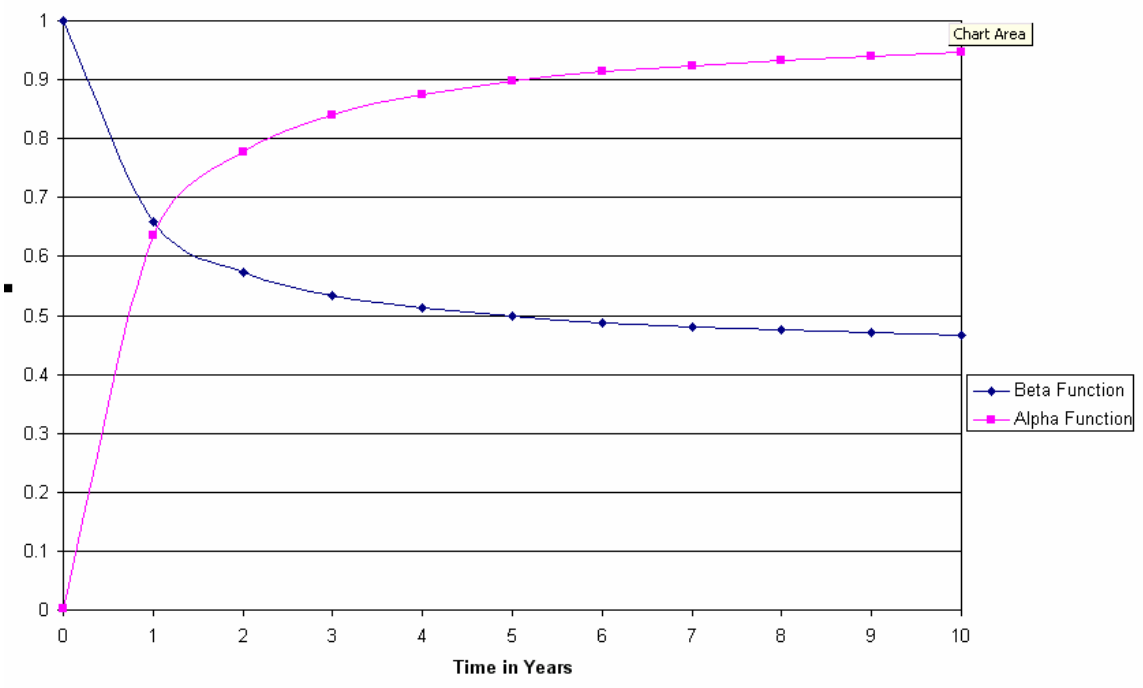


Figure F.2 Alpha and Beta Functions vs. Time

99% Oxygen Bottle Re-filler

Table F.5 TCI for 99% Oxygen Bottle Re-filler

Capital Investment for Portable Oxygen Device		
	Percent of Equipment Cost	
Direct Costs		
Purchased equipment delivered	100	\$17,000,000
Purchased-equipment installation	45	\$7,650,000
Instrumentation and controls	18	\$3,060,000
Piping	16	\$2,720,000
Electrical systems	10	\$1,700,000
Buildings	25	\$4,250,000
Yard Improvements	15	\$2,550,000
Service facilities	40	\$6,800,000
Total direct plant cost	269	\$45,730,000
Indirect costs		
Engineering and supervision	33	\$5,610,000
Construction expenses	39	\$6,630,000
Legal expenses	4	\$680,000
Contractor's fee	17	\$2,890,000
Contingency	35	\$5,950,000
Total indirect plant cost	128	\$21,760,000
Fixed Capital Investment	397	\$67,490,000
Working Capital (15% of TCI)	70	\$11,910,000
Total Capital Investment	467	\$79,400,000

Table F.6 NPW for 99%Oxygen Bottle Refiller

Year,n	Demand	Sales (\$/year)	Product Cost	Gross Earnings	Depreciation	Taxes	Net Profit	Cash Flow	CFn/((1+r)^n)
1	11	2.E+05	1.E+07	-1.E+07	7.E+06	7.E+03	-2.E+07	-1.E+07	-9.E+06
2	2,959	6.E+07	3.E+07	3.E+07	7.E+06	2.E+06	2.E+07	3.E+07	2.E+07
3	3,250	6.E+07	3.E+07	3.E+07	7.E+06	2.E+06	3.E+07	3.E+07	2.E+07
4	3,383	6.E+07	3.E+07	3.E+07	7.E+06	2.E+06	3.E+07	3.E+07	2.E+07
5	3,461	6.E+07	3.E+07	3.E+07	7.E+06	2.E+06	3.E+07	3.E+07	2.E+07
6	3,514	7.E+07	3.E+07	4.E+07	7.E+06	2.E+06	3.E+07	3.E+07	2.E+07
7	3,552	7.E+07	3.E+07	4.E+07	7.E+06	2.E+06	3.E+07	3.E+07	2.E+07
8	3,581	7.E+07	3.E+07	4.E+07	7.E+06	2.E+06	3.E+07	3.E+07	2.E+07
9	3,604	7.E+07	3.E+07	4.E+07	7.E+06	2.E+06	3.E+07	3.E+07	1.E+07
10	3,622	7.E+07	3.E+07	4.E+07	7.E+06	2.E+06	3.E+07	3.E+07	1.E+07
								NPW	\$74,117,579

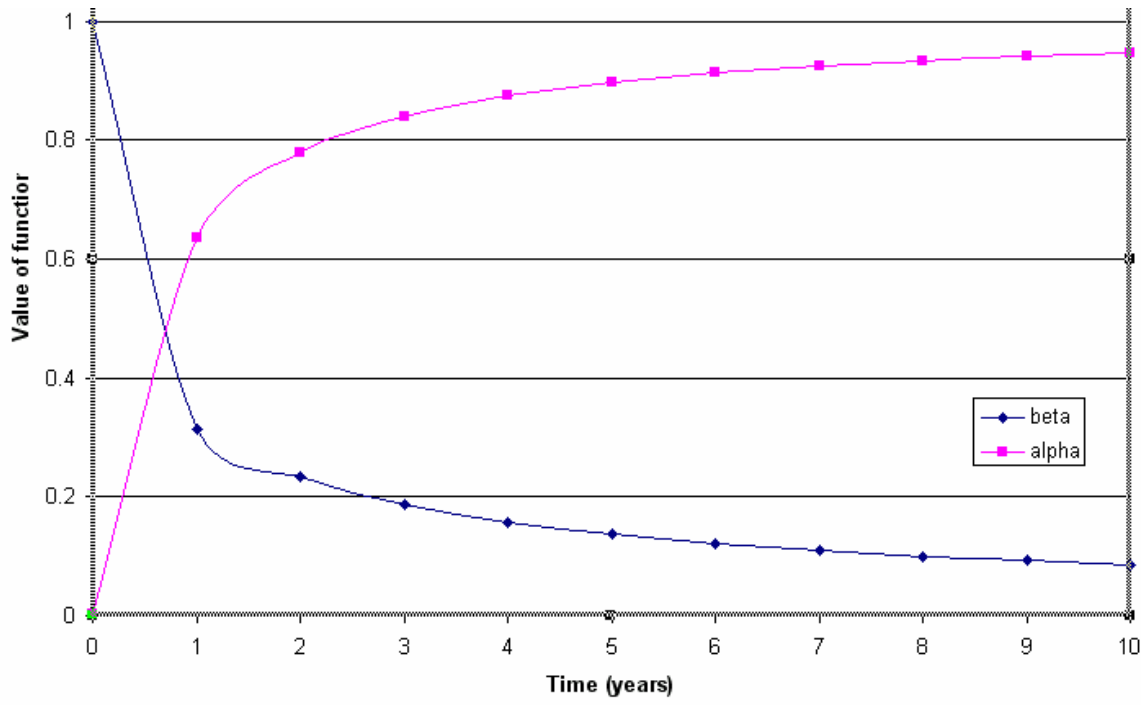


Figure F.3 Alpha and Beta vs. Time for 99% Oxygen Bottle Re-filler